Study of the eco-morphological diversification of the family Iphimediidae (Crustacea, Amphipoda) on the Antarctic continental shelf

Auteur : Martinez Soares, Pablo
Promoteur(s) : Verheye, Marie
Faculté : Faculté des Sciences
Diplôme : Master en océanographie, à finalité approfondie
Année académique : 2020-2021
URI/URL : http://hdl.handle.net/2268.2/12855

Université de Liège, Faculté des Sciences

Muséum National d'Histoire Naturelle, Paris

Study of the eco-morphological diversification of the family Iphimediidae (Crustacea, Amphipoda) on the Antarctic continental shelf

Pablo Martinez Soares

Mémoire présenté en vue de l'obtention du diplôme de Master en Océanographie

Promotrice : Marie Verheye

Lecteurs : Phillipe Compere

Patrick Dauby

Bruno Delille

Année académique 2020-2021

Acknowledgments

I wanted to thank my supervisor, Dr. Marie Verheye, for this amazing opportunity. Thank you very much for all the teaching, the time invested in explaining all sorts of software and concepts and helping me with the segmentations. Thanks for the comments on my many drafts, the support and the optimism at the end.

I thank my lectors, Pr. Philippe Compère, Pr. Patrick Dauby and Pr. Bruno Delille for being part of my jury and reading my work.

I thank Pr. Anthony Herrel, head of FunEvol at the MNHN, for welcoming me in his team and his precious feedback on my results and discussion.

A very special thanks to Jeanne Buffet for her council, reading over my work and helping me with the figures. Thanks for the support, the encouragements, the hugs and generally just being there for me.

A final thanks to my family, for their support and helping me through these sometimes difficult times.

Abstract

The Antarctic shelf and the fauna living on it have been moulded by millions of years of extreme seasonality, extreme isolation, extreme cold and recurrent glacial periods. Iphimediidae is a family of amphipods well-represented on the Antarctic shelf with at least 13 genera and 46 species. Recent molecular studies have shown that these are monophyletic and are in fact for the most part species complexes. Iphimediidae present a large diversity in mouthpart morphologies. Their mandibles are marked by the positioning of the incisor along the median line enabling it to cut in a frontal plane like scissors. This might have been one of the major reasons for their ecological success. Conversely, the basis of the maxilliped seems to conserve its general morphology across taxa. Using a time calibrated phylogeny of the family from a recent study, isotopic data as a proxy for the trophic niche and geomorphometric data of the mandible and the maxilliped's basis from 50 putative species of Iphimediidae, this study set out to *(i)* explore the mouthparts' morphological diversity, *(ii)* study the relation between morphology and trophic ecology and *(iii)* analyse the evolution of the morphological traits along the phylogeny. For *(i)*, measures of phylogenetic signal are significant but low for both mouthparts indicating variability among related species. The phylomorphospaces indicates that different clades present different modes of diversification. It also indicates that many species cluster in a limited region of morphospace. For *(ii)*, using a MANOVA in a penalized likelihood framework to test if isotopic data could explain morphology no significant results were obtained suggesting a one-to-many situation in mandibles and a many-to-one for the maxilliped's basis. For *(iii)*, fitting models of trait evolution to our data, we find that the Ornstein-Uhlenbeck is the best fitting model where morphology is driven by selection towards an optimum. A study of disparity through time finds that disparity is higher than expected under a stochastic model. The high diversification within subclades is likely due to recurrent extinction and allopatric speciation events due to icesheet advance and isolation of species in refugia.

Abstract (fr)

Le plateau continental antarctique et la faune qui y vit ont été façonnés par des millions d'années de saisonnalité, d'isolement, de froid extrêmes et périodes glaciaires récurrentes. Les Iphimediidae sont une famille d'amphipodes bien représentée en antarctique avec au moins 13 genres et 46 espèces. Des études moléculaires récentes ont montré que celles-ci sont monophylétiques et sont en fait pour la plupart des complexes d'espèces. Les Iphimediidae présentent une grande diversité morphologique des pièces buccales. Leurs mandibules sont marquées par l'incisive positionné le long de la ligne médiane lui permettant de couper dans un plan frontal comme des ciseaux. Ceci pourrait être l'une des raisons majeures du succès écologique de cette famille. A l'inverse, la base du maxillipède semble conserver sa morphologie générale à travers les taxons. En utilisant une phylogénie calibrée provenant d'une étude récente, des données isotopiques comme proxy pour la niche trophique et des données géomorphométriques de la mandibule et de la base du maxillipède de 50 espèces putatives d'Iphimediidae, cette étude a pour but (i) d'explorer la diversité morphologique des pièces buccales, (ii) d'étudier la relation entre la morphologie et l'écologie trophique et (iii) d'analyser l'évolution des traits morphologiques le long de la phylogénie. Pour (i), les mesures du signal phylogénétique sont significatives mais faibles pour les deux pièces buccales indiquant de la variabilité entre espèces apparentées. Les phylomorphoespaces indiquent que différents clades présentent différents modes de diversification. Il indique également que de nombreuses espèces se regroupent dans une région limitée du morphoespace. Pour (ii), en utilisant une MANOVA dans un cadre de vraisemblance pénalisée pour tester si les données isotopiques pourraient expliquer la morphologie, aucun résultat significatif n'a été obtenu, suggérant une situation d’un à plusieurs dans les mandibules et de plusieurs à un pour la base du maxillipède. En ce qui concerne (iii), testant différents modèles d'évolution des caractères, nous constatons que le modèle d'Ornstein-Uhlenbeck est le mieux adapté, la morphologie étant dirigée par la sélection vers un optimum. Une étude de la disparité dans le temps montre que la disparité est plus élevée que prévu dans un modèle stochastique. La forte diversification au sein des sous-clades est probablement due à des extinctions récurrentes et à des événements de spéciation allopatrique dus à l'avancée de la calotte glaciaire et à l'isolement des espèces dans des refuges.

Table of content

C*onformément aux règles imposées à la rédaction, ce mémoire ne doit pas dépasser 50 pages, rédigées en Times 12 ou équivalent*

1 Introduction

1.1 Antarctica and the Southern Ocean

1.1.1 Modern physical setting

Antarctica is the continent on the South Pole of our planet (*Fig. 1*). As explained by David and Saucède (2015), about 14 x10^6 km² of land constitute the most isolated continent on earth, 1000 km away from the closest continent, South America. It is covered by an in average 2200 m thick ice sheet, 30 x10^6 km³ of ice (David and Saucède, 2015). The Southern Ocean (SO) is bordered to the south by the Antarctic Continent and to the north by the 60° parallel south (David and Saucède, 2015). For scientists, the SO *sensu stricto* has its northern limit at thePolar Front, where westerlies meet the polar easterlies, and covers thus nearly 35 x10^6 km^2 (or about 10 % of our planet's ocean surface) which makes it the fourth largest ocean (David and Saucède, 2015; De Broyer et al., 2014). Similarly imposing, the Antarctic continental shelf covers 4.6 x10^6 km², 11 % of all continental shelves on Earth (David and Saucède, 2015).

Due to glacial erosion and the depression caused by isostatic loading by the ice sheet, the continental shelf is deep with a mean depth of 450 m and maximum of 1000 m (Post et al., 2014). The shelf width varies highly: the Ross and Weddell Seas extend up to 1000 km from the continental margin to the shelf edge and Dronning Maud Land'shelf in East Antarctica extends only 15 km (Post et al., 2014).

The Antarctic marine ecosystems are influenced by the currents. The SO being zonally continuous around the globe, it allows for the existence of the largest and most powerful current on Earth, the Antarctic Circumpolar Current (ACC; Post et al., 2014). The ACC flows from west to east and is driven by a combination of wind stress from the westerlies and the change in density of the cooling water masses in the sub-polar regions (Post et al., 2014). This current is essential for the global thermohaline circulation as it transfers heat, nutrients, CO_2 and O_2 around the globe (Post et al., 2014). The east wind around the continent drives two currents flowing westward notably the Antarctic Coastal Current (ACoC), following the Antarctic coastline over the shelf (Post et al., 2014).

Laying south of the Antarctic polar circle (latitude 66° 33' S), there is permanent day during summer and permanent night during winter, making light a limited resource in the water column during half the year (David and Saucède, 2015). Yet, even during summer, the solar angle remains low, cloudy weather is common and the presence of sea ice hampers the transmission of photons to the underlying water column (David and Saucède, 2015).

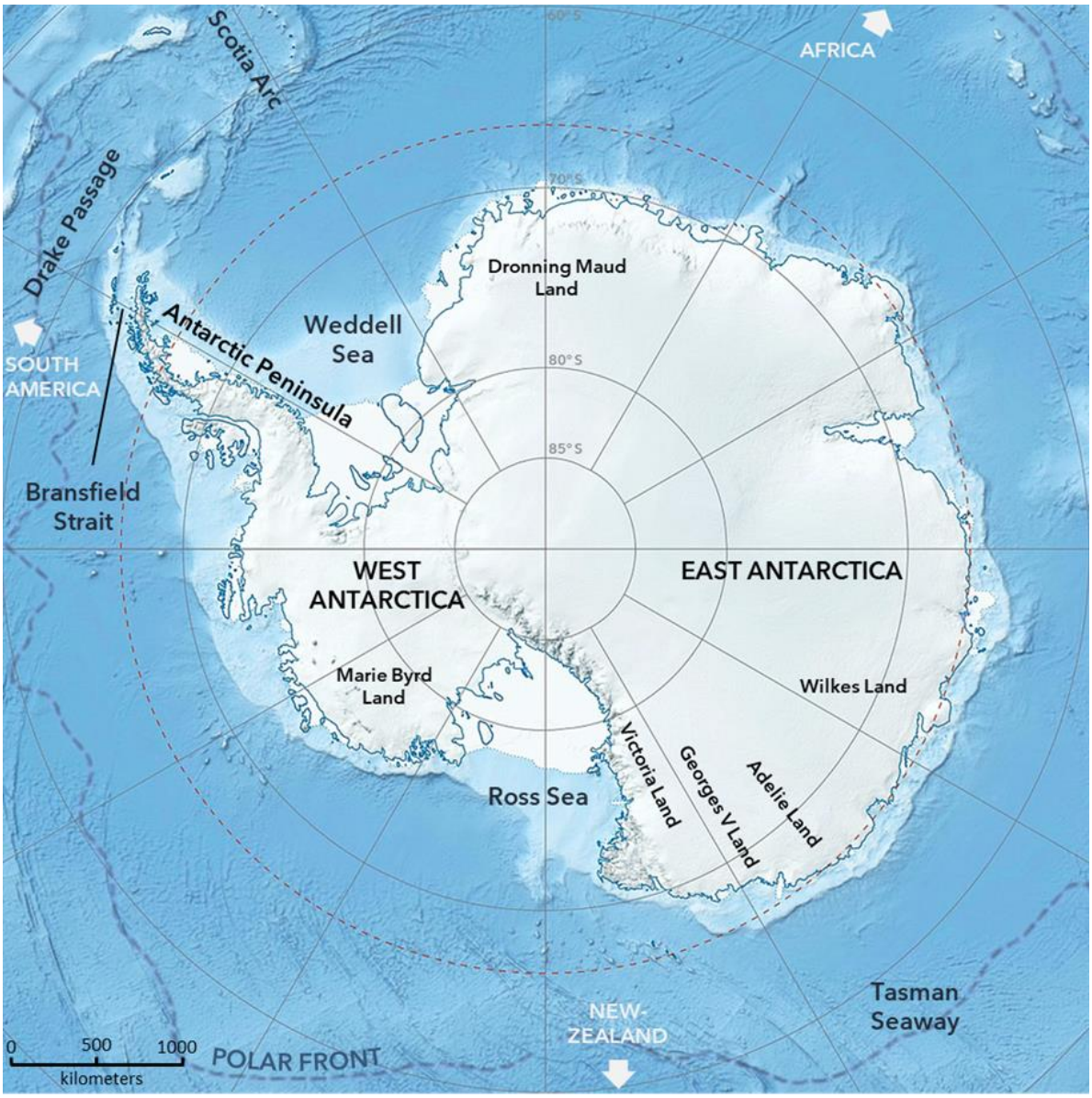

Figure 1 **:** Map of Antarctica centred on the South Pole (azimuthal equidistant projection). White surface indicates the modern minimum extant of the ice shelf; light blue indicates the continental shelf; arrows indicate the direction of the nearest landmass; red dotted line represents the Antarctic circle; blue dotted line presents the approximate position of the Polar Front.

One could not speak of the SO without mentioning the role of ice in this environment. At a salt content of 35 g L^{-1}, water starts freezing at -1.9° C. The Antarctic sea ice extent is massive with a minimum extent of about 3 x10^6 km² in February (austral summer) and maximum extent of about 18 x10^6 km² in September (austral winter) at the end of the growth season (Post et al., 2014).

1.1.2 Historical setting

Antarctica, as part of the supercontinent Gondwana, reached the Earth's south pole about 120 Ma during the Jurassic (Crame, 2014; Verheye, 2017). Starting during the Jurassic, Gondwana split: first, East separated from West Gondwana, leading to the separation of the Antarctic plates

with the African continent, then happened the separation with the Indian sub-continent during the late Jurassic followed by the separation of the Antarctica-Australia block during the Late Cretaceous (Crame, 2014). It seems that the Tasmanian Gateway, while already forming, was still blocked at that time and only opened during the Eocene probably about 50 Ma leading to the almost complete isolation of Antarctica (Crame, 2014; Lawver et al., 2014). During the Eocene, about 50 Ma, the Drake Passage, separation between the Antarctic Peninsula and South America, began to form (Lawver et al., 2014; Livermore et al., 2005). It is not clear when the deep-water passage here appeared, yet, it has often been dated at the Eocene-Oligocene boundary about 34 Ma (Crame, 2014; Verheye, 2017). It is suggested that the deep-sea ACC started during the Oligocene and would have had no barriers by the middle Miocene, about 10 Ma (Lagabrielle et al., 2009; Lawver et al., 2014).

As stated above, Antarctica has been placed on the south pole since the Cretaceous during which estimated "supergreenhouse" conditions transitioned to a cooler greenhouse environment, possibly driven by lower CO_2 levels in the atmosphere (Bowman et al., 2013; Linnert et al., 2014; *Fig.* 2). Follows the Cretaceous-Paleogene (K-Pg) mass extinction, probably in two pulses and hypothetically linked to a rapid temperature increase, itself followed by cooler climate persisting during the Paleocene until the new greenhouse period of the Eocene (Bowman et al., 2016; Petersen et al., 2016). All through the Eocene, ephemeral ice-sheets might have existed on elevations (Miller et al., 2008). Earth enters icehouse conditions in the earliest Oligocene (~33.5 Ma; Crame, 2014; Miller et al., 2008). Here, even though it might have happened in individual smaller steps, global oceans experience the steepest temperature fall of the Cenozoic; ice sheets might have reached the coast for the first time and Antarctica might have been nearly fully glaciated (Crame, 2018; Miller et al., 2008). Up to the Miocene there is a mixed phase of radiation and extinction due to glacial expansion and early Miocene warming (Crame, 2018; Wilson et al., 2008). Then, during the Middle Miocene (~15 Ma) occurs a warm interval: the Middle Miocene Climatic Optimum (MMCO; Crame, 2014; Gasson et al., 2016; Steinthorsdottir et al., 2021). Here, the Antarctic ice sheet reached a minimum, yet the shelf had already a stable core and the West Antarctic Ice Sheet (WAIS) might have periodically extended until the continental shelf edge in the Ross Sea during the late-Middle Miocene (Gasson et al., 2016; Steinthorsdottir et al., 2021). After the MMCO follows a long intense cooling into the Late Miocene (~14 Ma) leading to increased ice sheets (Crame, 2018; Verheye, 2017). This Mid-Miocene climatic transition (MMCT), the second abruptest fall in global ocean temperature of the Cenozoic, has been suggested as linked to the development of the ACC but

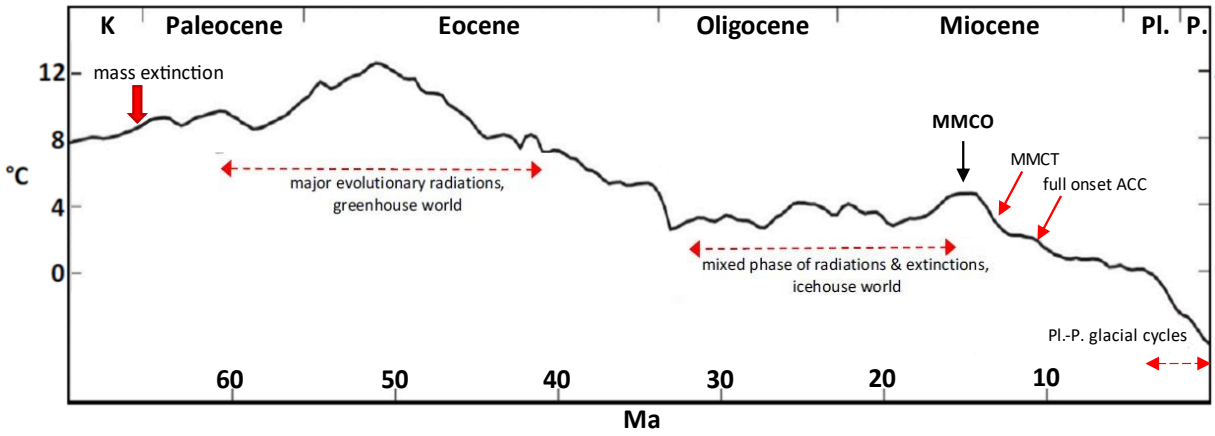

Figure 2 *:* Key stages in the evolution of the Antarctic marine fauna through the Cenozoic era are superimposed on the deep-sea palaeotemperature curve developed by Zachos et al. (2008) and Hansen, Sato, Russell, and Kharecha (2013). It should be noted that shelf-depth palaeotemperatures do not necessarily track those of the deep-sea precisely. ACC, Antarctic Circumpolar Current; K, Cretaceous; MMCO, Middle Miocene Climatic Optimum; MMCT, Mid-Miocene climatic transition; Pl, Pliocene; P, Pleistocene. Adapted from Crame (2018).

might also be due to carbon cycle changes (Burls et al., 2021; Crame, 2018; Lagabrielle et al., 2009). Then, during the Pliocene we once again find a warm interval bracketed by colder climate at about 3.1 Ma (Dolan et al., 2018). The extent of the Antarctic ice shelf during this period is still uncertain; it has been however suggested that there might have been periods without WAIS and the East Antarctic Ice Shelf (EAIS) margin might have been very dynamic; yet modelling remains difficult (Dolan et al., 2018). The Pleistocene is marked by repeated glacial progress across the continental shelf at glacial-interglacial timescales with margin retreat in the EAIS and probably at least one interglacial without WAIS (McKay et al., 2012; Pollard and DeConto, 2009; Wilson et al., 2018). The existence of 38 full glacial cycles, with ice sheets reaching the shelf break, has been estimated for the Ross Sea during this period of Plio-Pleistocene (Naish et al., 2009). About 15,000 yr ago, the Last Glacial Maximum, ice sheets reached the continental shelf edge before starting to retreat and reached near-modern extents about 3000 yr ago (Pollard & DeConto, 2009; Verheye, 2017).

1.1.3 Evolutionary Setting

Some SO organisms find their roots in the Mesozoic, perhaps even the Late Paleozoic (Crame, 2018). Yet, for many taxa, an incomplete fossil record makes it difficult to assess when they reached high latitudes (Crame, 2018). As shown in Seymour Island's stratigraphy, the K-Pg extinction meant the demise of about 61 % of all SO species and 43 % of the genera (Crame, 2018; Petersen et al., 2016). Follows a period of low diversity-high abundance assemblages; the restoration of pre-K-Pg diversity levels might have taken some 3 Myr through a massive radiation (Crame, 2018). The fact that certain groups developed a distinct polar fauna during the Eocene greenhouse world indicates that there is more at play than just cold weather, and the

high seasonality of primary production due to light availability in these regions might play an important role as well (Crame, 2018). From the start of the MMCT on, a time of intensified glaciation, we observe increases in diversity for many modern Antarctic groups like whales, pinguins, seals, notothenioid fishes and invertebrates like some octopus clades, octocorals and amphipods (Crame, 2018; Verheye et al., 2017). Diversification events might have continued until today. It has been notably hypothesized that the Plio-Pleistocene glacial cycles could have increased diversification, leading to bursts of closely-related species (species complexes; Crame, 2018).

Indeed, during interglacial periods, scouring of the shelf and benthos eradication is only caused locally by grounding icebergs, perhaps even helping diversity in the long-term by creating environmental heterogeneity (Thatje et al., 2005). However, during glacial periods, ice sheets increase in size, lowering sea-levels, and extending grounded onto the continental shelf which likely destroys all life in their path (Thatje et al., 2005). Outer shelve areas, to which the ice sheets might not extend, are still possibly affected by icebergs, seasonal ice cover and glaciogenic debris pushed by the developing ice (Thatje et al., 2005). Diachronous ice sheet growing and deglaciation would allow benthic organisms to find refugia on unaffected shelfs and slopes, probably linked to polynyas (Allcock and Strugnell, 2012; Thatje et al., 2008, 2005). As the populations finding refuge are small, there is a strong reduction in genetic diversity, *i.e.* a bottleneck (Allcock and Strugnell, 2012). Genetic drift then has a larger impact on the gene pool; species without pelagic larvae or drifting stages and thus slow at recolonizing shelf areas are more affected since genetic drift has more time to impact their genetic diversity before secondary contact of isolated populations (Allcock and Strugnell, 2012). This can lead to allopatric speciation through reproductive isolation if enough time is given. The resulting species often remain morphologically similar, forming complexes of (pseudo-) cryptic species (Allcock and Strugnell, 2012). When the physiology allows resisting high pressure differences, some species with larger bathymetric ranges could also have found refugia on the surrounding slope or deep-sea (Allcock and Strugnell, 2012; Thatje et al., 2005).

1.1.4 Modern fauna

Millions of years of extreme environmental conditions have thus moulded the Antarctic fauna making the Antarctic benthic landscape rather peculiar. While abundant during the Eocene, there is nowadays absence or low taxonomic diversity of heterodont bivalves, decapods, teleost fishes and Chondrichthyes, which likely allowed the diversification of other groups like the now abundant amphipods, isopods, notothenioid fishes and pycnogonids (Crame, 2018; Post et

al., 2014). Regions with low ice impact can develop large three-dimensional assemblages of suspension-feeders like sponges, anemones, and soft corals which in turn provide habitat for other taxa like crinoids, bryozoans and brachiopods giving an archaic appearance to the benthos (Crame, 2014). Openings in the ice exposing the underlying water, *i.e.* polynyas as well as any type of fracture, are areas of high importance for the local fauna as the absence of ice allows primary production to happen during longer time periods (Post et al., 2014; Thatje et al., 2008). The inability of benthic organisms to escape ice scouring and recolonize quickly after ice retreat causes coastal and shallow water environments to host a poor diversity of species of low abundances and as ice disturbance diminishes with depth, biodiversity increases (Post et al., 2014). Like for the pelagic communities, benthic communities are affected by the light budget let through by ice as it regulates the primary production of benthic algae and affects the food availability for benthic suspension- and deposit- feeder (Post et al., 2014).

1.2 Amphipoda

1.2.1 Generalities

Amphipoda is an order in the superorder Peracarida in the class Malacostraca, the subphylum Crustacea and the Phylum Arthropoda (WoRMS - Amphipoda). It is one of the most diverse order of crustaceans (Lowry & Myers, 2017). It comprises six suborders (Pseudoingolfiellidea, Hyperiidea, Colomastigidea, Hyperiopsidea, Senticaudata, Amphilochidea) composed of 223 families, some 1618 genera and about 10,277 species recorded to this day (Lowry & Myers, 2017). They are ecologically very diverse; about 80 % are marine and estuarine, about 19 % live in fresh water environments and the remaining (all in Talitridira) are supralittoral (Lowry & Myers, 2017). The females brood their young in a marsupium (Lowry & Myers, 2017). The general attributes that differentiate them from other Peracarida are the sessile eyes, coxal gills, epimeral plates, uropods and their lack of carapace (Lowry & Myers, 2017). While the monophyly of Amphipoda (with Ingolfiellida as a sister order) is rather undisputed, the classification within the order is still subject to discussion and in need of further systematic studies (Lowry & Myers, 2013, 2017; Verheye et al., 2016).

While the general anatomy is maintained, body forms can be quite different in Amphipoda (Hayward and Ryland, 2017). They present a generally laterally compressed body (Hayward and Ryland, 2017). The body is formed by the head (technically a cephalothorax), the pereon (seven thoracic segments, each with a pair of appendages: the pereopods) and the pleon (six abdominal segments), the latter being divided into the pleosome (anterior three segments of the pleon, each with a pair of pleosomes, the first two often transformed into gnathopods) and the

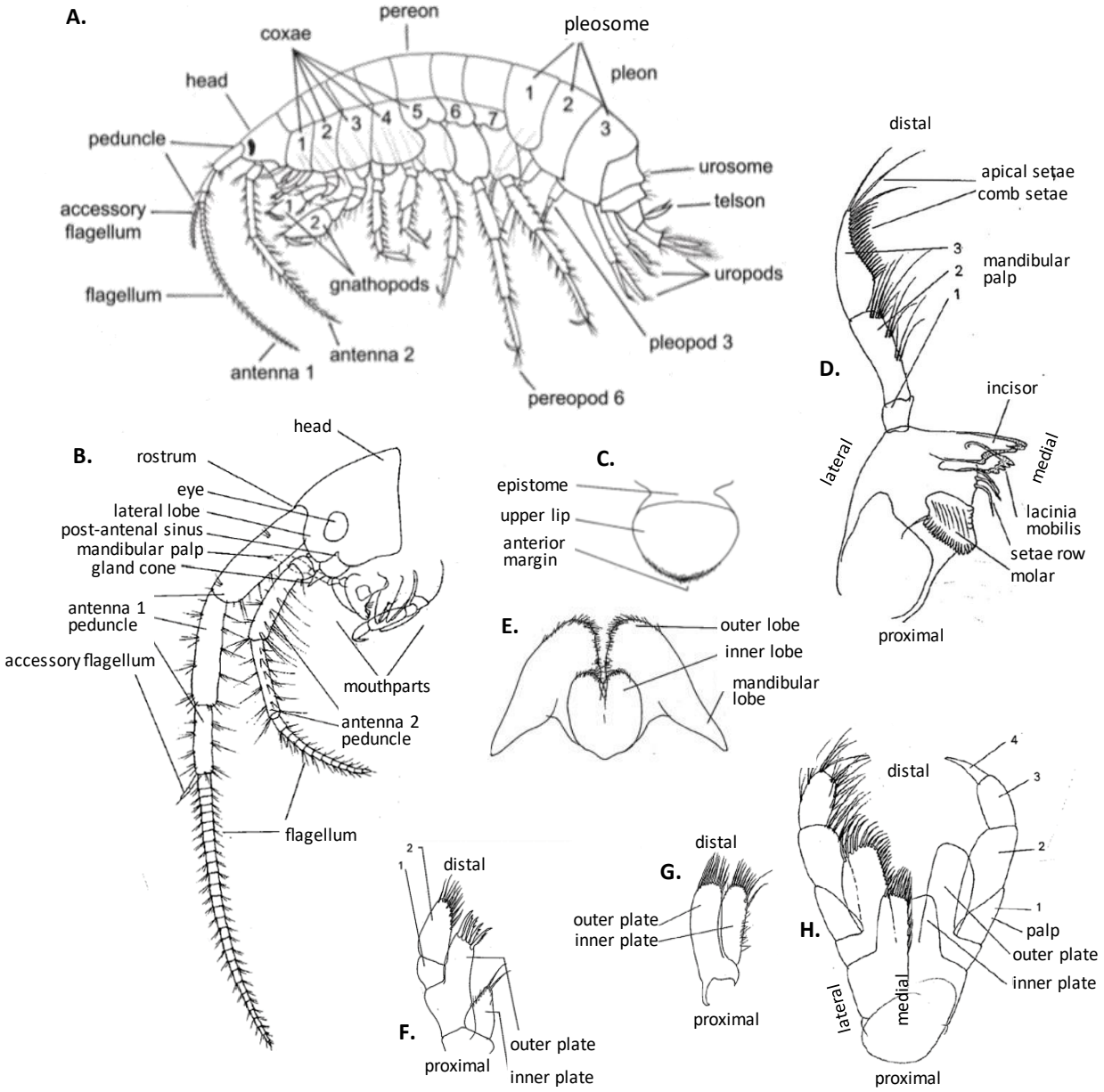

Figure 3: General anatomy of Amphipoda. A. Lateral view od whole body. B. Lateral view of the head. C. Anterior view of the upper lip. D. Anterior view of the mandible. E. Posterior view of the lower lip. F. Anterior view of the maxillule. G. Anterior view of the maxilla. H. Anterior view of the maxilliped. Adapted from Hayward & Ryland (2017) and Lincoln (1979).

urosome (posterior three segments of the pleon, each with a pair of urosomes; *Fig.* 3A). The terminal appendage, covering the anus, is the telson (Hayward and Ryland, 2017; Lincoln, 1979). Six pairs of appendages are present on the head: antennae 1, antennae 2, mandibles, maxillule, maxillae and maxillipeds (*Fig.* 3B). The latter four appendages together with the upper and lower lips (respectively anteriorly and posteriorly positioned to the mouth opening) form the mouthparts (Hayward and Ryland, 2017; Lincoln, 1979). The mandibles are the mouthparts closest to the mouth (*Fig.* 3D) followed by the maxillule, a small biramous appendage made from an outer and an inner plate with a small 1 or 2-articulate palp (Lincoln,

1979). Similarly, the smallest mouthpart, the maxilla, also possesses an inner and outer plate (Lincoln, 1979, *Fig.* 3G). The outermost and largest mouth appendages are the maxillipeds (see below; Lincoln, 1979, *Fig.* 3H).

1.2.2 Mandible and Maxilliped

The mandibles are used for cutting and grinding food. The basic amphipod mandible has a mandibular body (or coxa) generally compact and bears *(i)* an incisor (or incisor process) which is a (sometimes toothed) distal projection, classically oriented to cut in the transverse plane of the organism perpendicular to the long axis of the mandible, *(ii)* a molar (or molar process) projecting on the median margin of the mandibular body possessing usually different triturative surfaces to meet the molar of the opposite mandible in a rolling, crushing action, *(iii)* a setae row (or lifting spines) comprising strong, upward curved, sometimes serrated setae on the median margin between incisor and molar and which push food cut by the incisor towards the molars, *(iv)* a *lacinia mobilis* (lm) which is a flat, articulate and sometimes toothed plate, positioned close to the incisor and interdigitating with the lm of the other mandible, and *(v)* a palp of three articles which projects from the anterior side of the mandible and positions itself between the antennae (Mayer et al., 2013; Michel et al., 2020; Watling, 1993). The mandible is attached to the outside of the head through an articular membrane and moves through adductor and abductor muscles attached on the proximal end of the mandible body (Coleman, 2002; Watling, 1993). These mandible adductors, responsible for biting, are the most powerful muscles in the cephalothorax and are inserted on the dorsal side of the cephalothorax capsule and on a thick tendon on the median proximal margin of the mandibular body (Coleman, 2002). The abductor muscles connect to an antero-proximal process (or apophyse). On the lateral and antero-proximal margin (at the base of the process) there are two pivot points allowing for the rotation of the mandible along the cephalothorax (Mayer et al., 2013). Usually, when closing, the right incisor enters the gap between the left incisor and the left lm acting as a double edged scissor (Mayer et al., 2013).Through an interplay between the right mandible's rotation, both lms and both setae rows, the food is pushed towards the molars where it is grinded and eventually pushed towards the foregut (Mayer et al., 2013).

The basic mandibular form with compact body, toothed incisor, a lm and a columnar molar designed for crushing is often associated to detritivory or deposit feeding (Michel et al., 2020). Changes to this basic morphological plan are abundant and usually encompass an elongation of the coxa, changes in width, dentition and orientation of the incisor, reduction of the molar and reduction to complete loss of the setae row (Watling, 1993). Thus, filter-feeders tend to keep

this morphology but increase their setation. Detritus-feeders can have stronger and numerous dentations on the incisor in addition to increased molar grinding surface and cuspidate and teethed setae on maxilla and maxilliped for scraping off food particles. Predators have generally enlarged, toothless and sharp incisors; those feeding on soft preys tend to have reduced molars, while feeding on hard crustaceans will lead to molars with a more triturative surface. Highly adapted scavengers can have wide and sharp, toothless incisors to bite off large pieces of carrion associated with large conical molars to push food into the foregut. Facultative scavengers show sometimes slender incisors and lower triturative surface. Herbivores have stout and sharp incisors with well-developed rasp-like molars (Michel et al., 2020).

The head in amphipods is actually a cephalothorax and the maxilliped is actually the modified appendages of the first segment of the amphipod's thorax (Coleman, 2002; Lincoln, 1979). The structure is thus similar to that of any other appendage with a coxa, usually fused, a basis often partially fused and with a large modified endite also called the inner plate, an ischium with a large modified endite too named the outer plate, and a palp usually composed of the merus, carpus, propodus and dactylus but that can be more or less reduced in its number of segments (Mayer et al., 2009). Not much is known about the function of the maxilliped. It is generally large enough to cover the other mouthparts and is thought to help hold the food in the mouth area with the outer plates and palps and pushing it towards the mandibles with the inner plate (Charles Olivier Coleman, 1989; Coleman, 1991; Dennell, 1933; Mayer et al., 2009). The seta of the plates and palps could be used to filter food particles from the water column or scraping them from surfaces and the palps could perhaps directly be used to capture food (Coleman, 1989a; Coleman, 1991; Mayer et al., 2009; Watling and Thiel, 2013). Morphological diversity in this appendage exists: palps, inner plates and outer plates can be vestigial or absent, the inner plates can be medially fused but are generally subrectangular and the outer plates can strongly vary specially in size and folding (Lincoln, 1979; Lowry and Myers, 2013).

1.2.3 Southern Ocean Amphipoda

Amphipods are the second most speciose macrobenthic group in the Southern Ocean after Gastropoda (De Broyer and Jazdzewska, 2014). As of 2014, 564 species with 66% of species endemism were described from regions south of the Polar Front (De Broyer and Jazdzewska, 2014). Most species come from the super-families Lysianassoidea and Eusiroidea, and the families Stenothoidea, Ischyroceridae, Iphimediidae, Phoxocephalidae and Epimeriidae (De Broyer and Jazdzewska, 2014). Yet, this number is constantly increasing due to new

identifications and molecular studies discovering (pseudo-) cryptic species (De Broyer and Jazdzewska, 2014; Verheye, 2017).

Amphipods are nearly ubiquitous in the communities of the SO. They have been described in different habitat types; specially the epibenthos is composed of a variety of microhabitats and is thereby very species-rich (Dauby et al., 2001; De Broyer et al., 2001). Amphipods are characterized by a variety of lifestyles: ice-associated dwellers, (bentho-) pelagic swimmers, benthic crawlers, walkers, burrowers, borers or inquilines in/on different vertebrates or invertebrates (living for example with sponges, ascidians, and hydrozoans or inside salps or coelenterates) or living and feeding as parasites on cetacean skin (Dauby et al., 2001a). They are also a key component of the SO food web being prey for fish, birds and marine mammals (Dauby et al., 2001a, 2001b). Isotopic studies show that benthic and pelagic amphipods cover a wide trophic spectrum in the Weddell Sea with diverse feeding strategies (Nyssen et al., 2005, 2002). Thus, we find micro- and macrophagy, herbivory, predation, browsing, necrophagy, as well as suspension- and deposit-feeding (Patrick Dauby et al., 2001). Many amphipods have a broad spectrum diet allowing them to benefit from whatever is available (Patrick Dauby et al., 2001; Michel et al., 2020). This might be linked to the high seasonality of SO productivity, where winter conditions are associated with food scarcity compared to the spring-summer blooms (Patrick Dauby et al., 2001).

1.2.4 Southern Ocean Iphimediidae

From the 15 accepted genera and 108 accepted species of Iphimediidae 13 genera and 46 species occur in the Antarctic and sub-Antarctic regions (Lowry and Myers, 2017; RAMS - Iphimediidae Boeck, 1871; WoRMS - Iphimediidae Boeck, 1871). In Iphimediidae, the body is laterally compressed, possesses dorsal teeth and a well-developed rostrum (Coleman and Barnard, 1991; Hayward and Ryland, 2017). Typically, the last pereonite and all three pleonites segments possess paired teeth on their dorsal side (Coleman and Barnard, 1991; Hayward and Ryland, 2017). The mouthparts form a conical bundle pointing ventrally (Coleman and Barnard, 1991; Hayward and Ryland, 2017). The mandibles' incisors are highly variable in shape, the molar is absent or strongly reduced into a fleshy lobe, the 3-articulate palp is always present (Coleman and Barnard, 1991; Hayward and Ryland, 2017). They have changed the orientation of the incisors' cutting plane: instead of being positioned transversally and cutting horizontally, the incisors have a sagittal position, along the mandibular body's main axis, cutting in a vertical plane like scissors (Watling, 1993; Watling and Thurston, 1989; *Fig*. 4).

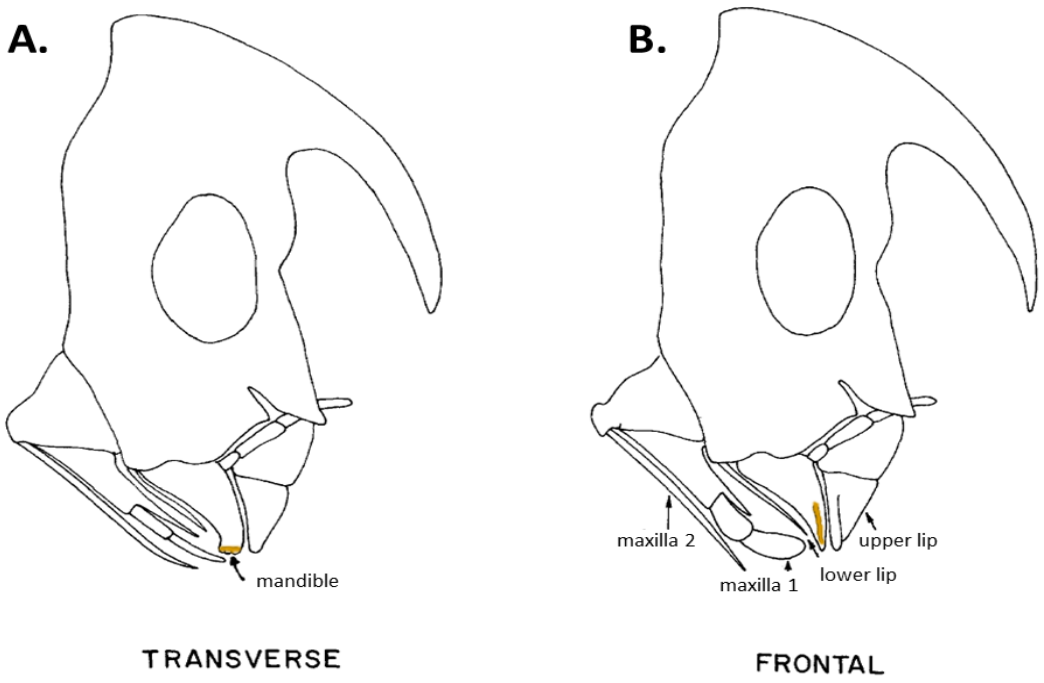

***Figure 4*:** Diagrammatic representation of the arrangement of the appendages in the mouth field of an amphipod. In A, the mandible incisor cutting surface is oriented in the horizontal transverse plane, whereas in B, it is oriented in the vertical frontal plane. The incisor cutting surface is indicated by the brown line on the mandible. Adapted from Watling and Thurston (1989)

Not much is known about the ecology of Antarctic Iphimediidae. They seem to be mostly walker-climbers, moving slowly on their last three pairs of pereopods, rarely swimming, and seem to live in the lower epibenthos on the shelf (De Broyer et al., 2001). While the bulk of Weddell Sea amphipod diets are carcasses, crustaceans and planktonic particles, Iphimediidae appears to be composed of species with specialized predatory feeding habits (Patrick Dauby et al., 2001). Their high diversity in mouthpart morphology suggests that they all have very distinct food preferences (Coleman, 1989).

Not much is known about the ecology of the 100+ species and current knowledge comes from large and common Antarctic shelf species that are *Echiniphimedia hodgsoni*, *Gnathiphimedia mandibularis*, *Iphimediella cyclogena*, *Maxilliphimedia longipes* and *Anchiphimedia dorsalis* (Coleman, 1989a, 1989b; Coleman, 1991; Dauby et al., 2001; De Broyer et al., 2001; Graeve et al., 2001; Michel et al., 2020; Nyssen et al., 2005).

E. hodgsoni has slender asymmetrical mandibles with strong *lacinia mobilis*, especially the right one, positioned parallel to the broad, smooth incisor which allows for a very effective cutting process (Coleman, 1989a). The inner plate of the maxilliped has setae all along its margin. This species appears to prefer living at the external surface of sponges and sometimes bryozoans, often gathering together and motionless or moving slowly (De Broyer et al., 2001). Gut content analysis revealed a lot of poriferan spicules probably from the family Chalinidae or Niphatidae suggesting that those sponges are their main food source (Patrick Dauby et al.,

2001). They do not contain a lot of storage lipids probably because sponges are a common all-year round available resource on the Antarctic shelf (Graeve et al., 2001). Some fatty acids found in unidentifiable organic matter in its gut suggests the consumption of diatoms or prey feeding on diatoms (Graeve et al., 2001). Similar observations have been done for *E. scotti* (De Broyer et al., 2001). Stable isotope analysis (based on n = 2) found $\delta^{15}N$ ratios of 10.6 ± 1.8 ‰ (and $\delta^{13}C$ of –24.4 ± 1.3 ‰) which is indicative of a rather high trophic position compared to other amphipods in the study (Nyssen et al., 2005). This could be due to high $\delta^{15}N$ in sponges through the consumption of sympagic organic matter or resuspended matter passed through important microbial loops (Nyssen et al., 2002).

G. mandibularis is associated with calcareous bryozoan colonies and more seldom with sponges, at least in aquaria (De Broyer et al., 2001). Their gut content suggests that their primary food source are mainly Cyclostomata bryozoans (78 %) and to a far lesser extent poriferans, and even ophiuroids in one individual (Coleman, 1989b; Dauby et al., 2001). Their mandibles are unique in Amphipoda in that the incisive is flat, without teeth and distally rounded and thus adapted for crushing hard food items (Coleman, 1989b; *Fig.* 5A). It crushes parts of the bryozoan colony, ingesting fragments consisting of several zooids and digesting the soft tissues in its foregut (Coleman, 1989b).

For *I. cyclogena, o*ssicles in their gut content have shown that their diet might be composed to a large part of holothurian tissue (about 70%) and to a smaller part of polychaetes (20%) and unidentified organic matter (Patrick Dauby et al., 2001; Nyssen et al., 2002). It has been shown to have high $\delta^{15}N$ ratios of 11.2 ± 0.5 ‰ (and $\delta^{13}C$ of –25.9 ± 1.1 ‰; based on n = 5) indicating a rather high trophic position (Nyssen et al., 2002). Its mandibular body is elongated and has a narrow, toothed incisor and a long *lacinia mobilis* and a reduced fleshy molar (Michel et al., 2020; *Fig.* 5B). This is very different from the only other amphipod known to feed on tough holothurians, *Alexandrella schellenbergi* (Stilipedidae), which has stout and serrate incisors (Coleman, 1990; Michel et al., 2020). The difference in mandible shape could be explained by the change in cutting plane (Michel et al., 2020).

M. longipes, found at the surface of different substrates in aquaria, seems generally associated with cnidarians (De Broyer et al., 2001). The predominance of nematocysts typical for Hexacorallia and Hydrozoa in their gut content (about 70%) suggests that it mainly feeds on cnidarians, yet diatoms where found too (Patrick Dauby et al., 2001). This species has stout mandibles with very broad and toothed incisors and vestipolices gial molars (Coleman, 1989a; *Fig.* 5C). The maxilliped's inner plates are short and their setae smooth; the outer plates are

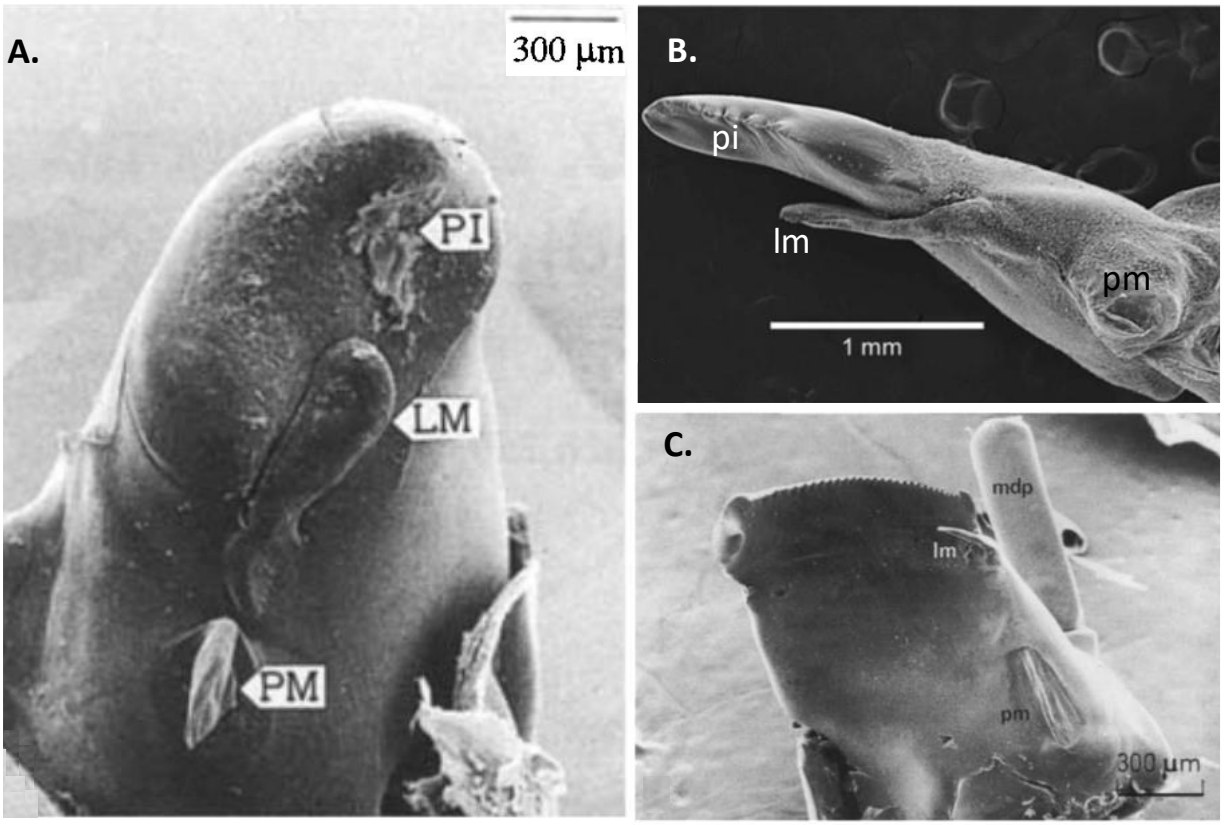

***Figure 5*:** Scanning electron microscopy pictures of mandible of several Iphimediidae. A. *Gnathiphimedia mandibularis*, left (Colemans, 1989b). B. *Iphimediella cyclogena*, right (Michel et al., 2020). C. *Maxilliphimedia longipes*, right (Colemans, 1989a). mdp, mandibular palp; lm, lacina mobilis; pi, incisor process ; pm, molar process.

broad and round covering all mouthparts (Coleman, 1989a). The large outer plate is also found in another cnidarian-feeder suggesting it might be practical for holding soft food (Coleman, 1989a). Compared to other species, the mouthparts are almost free of hair-like setae. The sparse setae present are smooth, which could be an adaptation for feeding on mucus-rich cnidarians, mucus which could entangle the setae (Coleman, 1989a).

A. dorsalis has a stout mandible with a smooth incisor and without spine row (Coleman, 1991). The maxilliped's inner plate has long distal setae. The outer plate has its laterodistal margin strongly folded orally with short setae along the margin (Coleman, 1991). Like *Pariphimedia* and *Paranchiphimedia*, it has a short maxilla 1 palp which could not be used for cleaning the feeding appendages or holding food like in other species (Coleman, 1991). The many and slender setae found on maxilla 1 and 2 could be used in co-ordination to brush food particles from sand grains like seen in *Bathyporeia* (Bathyporeiidae; Coleman, 1991). Sediment particles were found in the fore- and midgut with sand grains and fine detritus enclosed in a mucus-like matrix and some holothuroid ossicles in some individuals (Coleman, 1991). Its feeding habits seem unclear as the mandibles seem able to cut larger food pieces, but the gut content and the strong setation of the mouthparts would rather suggest detrital feeding (Coleman, 1991).

Thereby, at least for these species, Coleman's suggestion seems to apply as we do indeed observe high diversity in mouthpart morphology seemingly specialized to very specific food preferences as suggested.

1.2.5 Iphimediidae evolution in the Southern Ocean

Watling and Thurston (1989) suggested the major diversification of the family on the Antarctic shelf could have followed the isolation of the Antarctic shelf and coincided with the onset of Antarctic cooling around the Late Eocene. According to them, this radiation was characterized by a key innovation that is the reorientation of the incisor from the transversal to the sagittal plane. They suggested that the Antarctic shelf would have been and "evolutionary incubator" for this family and that they subsequently dispersed into the surrounding oceans as for *Labriphimedia* and *Iphimedia* species.

Recent molecular works by Verheye (2017), on which the present study is based, tends to confirm those early findings. The phylogeny based on mitochondrial cytochrome c oxidase subunit I (COI), nuclear 28S rDNA (28S) and Histone 3 (H3) shows that all (sub-) Antarctic species form a clade, while the sampled non-Antarctic species form another. The divergence between those two major clades was estimated at 44.11 Ma [95% confidence interval: 58.67 Ma – 30.88 Ma] and the most recent common ancestor of the Antarctic clade was estimated at 35.14 [46.41 – 25.22] Ma (Verheye, 2017). This period between the separation of both clades and the initial diversification of the Antarctic clade coincides with the onset of the cooling trend, starting across the early to middle Eocene boundary (ca. 48–49 Ma) and culminating by the onset of continental glaciations at the Eocene/Oligocene boundary (ca. 34 Ma; Verheye, 2017). As she states, the large confidence intervals do not allow to infer if the Antarctic clade diverged before or after the complete isolation of Antarctica. Nevertheless, these results show the geographical and/or environmental isolation of the (sub-) Antarctic Iphimediidae. The presence of (supposedly) the same species (*Pariphimedia normani* and *Iphimedia pacifica*, not sampled for this study) on both sides of the APF and the presence of the sister species *Labriphimedia pulchridentata* in the sub-Antarctic region and *L.* aff. *pulchridentata* on the Adelie Coast suggests dispersals from the Antarctic to the sub-Antarctic after the isolation of the continent (Verheye, 2017). Although the available bathymetric and geographical records for Iphimediidae are certainly not exhaustive, only *G. mandibularis*, *E. hodgsoni* and *I.* aff. g*eorgei* have been found on the slope at about 2000 m depth, and given that the mean depth of the Drake Passage is about 3400 m depth, it seems unlikely for Iphimediidae to disperse in and/or out of the Antarctic through the deep sea (Verheye, 2017). It seems more likely that long-distance

dispersion from and around the continent happened using macroalgal rafts, across and along the ACC and using the eddies formation at the Drake Passage to be transported north or south of the current (Verheye, 2017). As they seem to seldom swim and to be generally motionless on their substrate of choice, the raft hypothesis seems limited in explanatory power to species living on objects that could be used as rafts (Verheye, 2017). Furthermore, their adaptiveness to cold water environments might have limited the dispersal of the Antarctic clade to the North (Verheye, 2017).

Regarding the family's systematics, the genus *Iphimedia* appeared polyphyletic on her molecular phylogeny with *Iphimedia imparilabia* nested within the Antarctic species clade, while other *Iphimedia* species are non-Antarctic. *Gnatiphimedia* and *Iphimediella* were shown to be polyphyletic and, as both genera are defined (in part) by their incisor morphology, it suggests that similar incisor shapes evolved convergently, as species adapt to similar trophic niches. Moreover, she applied DNA-based species delimitation methods on the phylogeny and genetic distances suggest that the real diversity in this family is still unknown and underestimated, as many of the nominal species appeared to be species complexes.

As (sub-) Antarctic iphimediids arose in a Late Gondwanan to Early Antarctic cooling environment, the clade could have diversified due to ecological opportunities that arose with the extinction of cold-intolerant taxa and the emergence of rich suspension-feeder assemblages, following the extinction of durophagous predators during the Late Eocene – Oligocene (Verheye, 2017). The high diversity of newly available habitats could have led to a burst of lineage and eco-morphological diversification (Verheye, 2017). However, whereas a diversification slowdown, which would be indicative of a so-called early burst (EB) process, was detected by Verheye (2017) it was non-significant. According to the author, the non-significance of the detected slowdown in diversification could mean that *(i)* competition was high during the early history of their diversification thus, not enough opportunities where available for an adaptive radiation burst, *(ii)* sampling was insufficient or, *(iii)* high rates of extinction, due to the ice shelf locally erasing whole shelf communities during glacial maxima, eroded the EB signal. The lack of fossils makes it difficult to verify any hypothesis. An increase in diversification rate was detected at the base of the *Echiniphimedia* clade at about 3.86 [5.29 – 2.48] Ma which could be interpreted as burst of allopatric speciation as a result from repeated isolation of populations in ice-free refugia during glacial maxima as it has been interpreted for notothenioid fishes (Near et al., 2012; Verheye, 2017). This higher diversification rate could also be explained by the acquisition of a key innovation, *i.e.* the capacity to feed on sponges, a

seldomly used and abundant resource in the SO; however, not enough is known about the ecology of the different *Echiniphimedia* species (Verheye, 2017).

1.3 Objectives

Geometric morphometrics data capturing the shapes of two different mouthpieces, the mandible (mandibular body) and the maxilliped (inner plate), of specimens from 50 different species of Iphimediidae occurring in the Southern Ocean, were obtained. Combining these data with the pre-existing phylogeny of the family and stable isotope data ($\delta^{15}N$ and $\delta^{13}C$), we aimed to achieve the following goals:

(i) Explore the diversity of Iphimediidae's mandible and maxilliped shapes in an evolutionary context, using phylomorphospaces and a measure of the phylogenetic signal.

(ii) Study the relation between the trophic ecology (using stable isotopes as a proxy) and those mouthparts' shapes using Two Blocks – Partial least Squares and MANOVA in a penalized Likelihood framework.

(iii) Analyse the evolution of those morphological traits along the phylogeny, by calculating disparity-through-time plots and fitting our data to different trait evolution models.

2 Materials & Methods

2.1 Sampling

Figure 6 : Distribution of the sampling locations around Antarctica.

In total 50 amphipod specimens were used for this work. They were selected based on a previous DNA-based species delimitation analyses and cover nearly all delimited putative species (Verheye, 2017; see below). Sample list with attached metadata is provided as Supplementary table 1. Amphipods were collected during 11 different expeditions using Agassiz trawl (2 m width, 10 mm mesh), Beam trawl (3 m width, 12 mm mesh) and Rauschert dredge (60 cm width, 1 mm mesh).

Samples come mainly from the Weddell Sea (7 stations, 16 samples), the Adelie Land (12 stations, 14 samples) and the Bransfield Strait (12 stations, 13 samples), yet a few come from the Ross Sea (2 stations, 3 samples), Bouvet Island (1 stations, 1 samples), Macquarie ridge (1 stations, 1 samples), and the Drake Passage (2 stations, 2 samples; *Fig.* 6). Amphipods were stored in 96% EtOH and kept refrigerated at -20° C. Morphology-based identifications were done either directly on board or after the mission using notably Coleman (2007). Samples were coded with the three first letters of the genus, the three first letters of the species followed by an individual identification number (*e.g. Maxilliphimedia longipes* ID = O6: MAX_LON_O6).

2.2 Molecular phylogeny

In a previous study (Verheye, 2017), different methods of DNA-based species delimitation (GMYC, Fujisawa and Barraclough (2013) and bPTP, Zhang et al. (2013)) were applied on a molecular phylogeny of the family Iphimediidae based on COI, 28S and H3 genes (*cf.* figure 2 in Verheye, 2017). For the present study, we selected one specimen per putative species delimited by those two methods to reconstruct the time-calibrated tree.

BEAST2 (Bouckaert et al., 2014) on the CIPRES portal (Miller et al., 2010) was used to estimate divergence times under a Bayesian approach (Verheye, 2017). As no fossils nor unambiguous biogeographic events could be used to calibrate the tree, priors on rates of COI, 28S and H3 evolution based on rates inferred in previous studies were used. The prior rate of COI was set as a normal distribution with a mean of 0.018 substitutions site^{-1} My^{-1} and a standard deviation (SD) of 0.0043. This rate was previously inferred for *Pontogammarus* amphipods (Nahavandi et al., 2013). A normal prior with a mean of 0.003 substitutions site^{-1} My^{-1} and SD of 0.0007 was used for the 28S gene, a rate inferred for the *Gammarus balcanicus* complex (Mamos et al., 2016). Rates of H3 evolution are, to our knowledge, not available for amphipods. Therefore, the prior rate of H3 was set as a normal distribution with a mean of 0.0019 and SD of 0.0004, a rate inferred from freshwater crabs (Klaus et al., 2010). Three independent MCMC chains of 300 million generations each were run with a sampling frequency of 30 000 generations. For each chain, the first half of the trees were discarded as burn-in, and the remaining tree samples from all three chains were then combined. Convergence was assessed by trace plots in Tracer v.1.6. and the effective sampling size for all parameters was more than 200 (Rambaut et al., 2014). The maximum clade credibility tree showing the mean nodal height was generated by TreeAnnotator v1.8.0.

2.3 Isotopic data

The complexity of marine food web interactions can be summarized into two essential parameters : the diversity of producers sustaining the web and the trophic position of the different consumers (Michel et al., 2019; Post, 2002). Stable isotopes ratios of light biogenic elements like C, N and S are well-established trophic tracers used as proxies for both food web dimensions (Michel et al., 2019; Post, 2002). Indeed, these elements are found in lighter and heavier isotopic forms, the lighter often being more abundant, and their exact ratios will vary due to biological, geochemical and anthropogenic processes (McCutchan et al., 2003; Post, 2002). Hence, when an organism consumes a certain food item, assimilating it will make it incorporate its isotopes(McCutchan et al., 2003; Post, 2002). However, for each chemical or physical reaction, lighter isotopes of a certain element are more prone to undergo the reaction than heavier ones, *i.e.* isotopic fractionation, leading to an accumulation of heavier isotopes inside the consumer, *i.e.* trophic enrichment (McCutchan et al., 2003; Post, 2002). This happens at each metabolic process inside an organism, and fractionation might differ between different species, individuals and tissues (McCutchan et al., 2003; Post, 2002). Typically, $\delta^{15}N$ is used as measure of the ^{15}N:^{14}N ratio in an organisms (see below) and used to estimate its trophic position (McCutchan et al., 2003; Post, 2002; Quezada-Romegialli et al., 2018). Conversely, $\delta^{13}C$, the measure for the ^{13}C:^{12}C ratio (see below), varies less between trophic positions but can be used (often in combination with $\delta^{15}N$) to determine the food sources used and their proportions (McCutchan et al., 2003; Parnell et al., 2013; Post, 2002). This method has already been used to characterise the trophic position of amphipods (Michel et al., 2019, 2017; Nyssen et al., 2005, 2002; Søreide and Nygård, 2012).

Stable isotope data was collected by a former Msc student, Lory Léger-Bascou, Dr. Loïc Michel, Dr. Marie Verheye and Pr. Gilles Lepoint at the Oceanology laboratory of ULiège. One or several pleopod(s) were used per individual. Due to the small size and/or rarity of some iphimediid species, isotopic data could not be obtained for all samples used for the morphometric analyses. These were discarded in the ecomorphological analyses. Different batches of samples were processed, according to the weight of the collected tissue: <0.5 mg, between 0.5 and 1 mg and >1mg. Tissue samples were weighted and put in a tin capsule (6 x 4 mm). Additionally, were weighted and encapsulated : two blank capsules at the beginning of the batch and one at the end (~30 mg), one standard IAEA-N-2 (+20,4 ‰ ± 0,3 ‰, ammonium sulfate; IAEA) and one standard IAEA-C6 (-10,8 ‰ ± 0,3 ‰, sucrose; IAEA) at the beginning and the end of the batch (~0.5 mg), three glycine replicates at the beginning and the end of the batch plus one every 15 samples (similar weight as tissue samples), one seabass replicate at the

beginning and at the end of the batch plus one every 15 samples (similar weight as tissue samples). Between each sample, utensils were cleaned with acetone. Isotopic ratios were measured using continuous flow - elemental analysis - isotope ratio mass spectrometry (CF-EA-IRMS) with continuous helium flow. The EA used was a vario MICRO cube (Elementar Analysensysteme GMBH, Hanau, Germany) C-N-S elemental analyser associated to an isoprime preciseION (Elementar Analysensysteme GMBH, Hanau, Germany) as IRM spectrometer. δX (in ‰) is the deviation between isotopic ratios of ^{13}C:^{12}C and ^{15}N:^{14}N according to the formula: $\delta X = (R_{sample} - R_{standard})\ R_{standard}^{-1}$ x 1000 where X is the studied element and *R* is the isotopic ratio for the standard or sample respectively.

Spatial and temporal variation in SI values and variation in SI values of primary food sources at the baseline of food webs can lead to variation in individuals collected at different sampling locations and sampling periods which needs to be account for when compared (Le Bourg, 2020). This can be done by correction of mean values for each station but requires several specimens per station to have a good estimate of the mean per station (Le Bourg, 2020). Moreover, to diminish the impact of intraspecific variability, the SI values used to compare different species should be a mean value (usually from about 10 individuals per species). However, due to the sporadic nature of Antarctic sampling, in many cases, only one individual of a species was present in a station, making standardization difficult. Moreover, in many cases, non-sequenced specimens and their associated isotopic ratios could not be assigned to the DNA-based putative species, as the species complexes have not been studied morphologically yet (study in progress). To be certain that each isotopic ratio is associated with the rightful species, only the values obtained for the sequenced specimens of Fig. 7 were used. Thus, we got isotopic data for 37 of our 50 amphipods.

2.4 Computed tomography

Computed tomography (CT) is a non-invasive imaging technique (Du Plessis et al., 2017; Keklikoglou et al., 2019). In short, it works by capturing two-dimensional (2D) x-ray images of an object under different angles (often the x-ray source and detector are fixed and the objects, placed between both, rotates) which are then put together by a computer to create a digital three-dimensional (3D) reconstruction of the object (Du Plessis et al., 2017). When the resolution is in the micrometre range the method is called micro-computed tomography (µCT).

2.4.1 Sample preparation

Sample preparation for CT is minimal and requires only the fixation of the samples inside a falcon tube using agarose gel which solidifies around the specimen. Thus, up to seven amphipods (depending on their size) could be positioned inside a 12 cm-long tube. Samples from the MNHN collections were scanned at the technical platform Accès Scientifique à la Tomographie par Rayons X (AST-RX, MNHN, Paris) using a Phoenix v|tome|x L 240-180 (Baker Hughes Digital Solutions, Houston, Texas, U.S.A., maximal voxel resolution of 1 µm). The remaining samples were scanned at RBINS, Brussels, using an XRE UniTom (XRE NV (Tescan), Ghent, Belgium, maximal voxel resolution of 0.5 µm) for small samples (~0.5-2 cm) and a RX EasyTom 150 (RX Solutions, Chavanod, France, maximal voxel resolution of 4 µm but generally used at about 10 µm) for larger samples (~2-4 cm). Scans and image reconstruction were done by a specialized technician. The result was a folder containing a sequence of grey-scale slices of the specimen (generally about 1000 slices) all along the scanning axis (in TIF format).

2.4.2 3D reconstruction & segmentation

The slices were imported into *ImageJ* (version 2.35) and cropped to contain only the amphipod and thereby reduce file size. Contrast was adjusted and files were transformed to 8-bit format and saved as a new RAW file containing the whole sequence of slices.

For segmentation, the RAW sequence was imported into AVIZO (version 8.1, Thermo Fisher Scientific, Waltham, U.S.A.), then labels were added using the label field editor. A label consists in a grid indicating for each voxel the region it belongs to, allowing to separate and classify objects in an image. Since we were to use Biomedisa for the segmentation (see below) pre-segmentation was done on approximately every tenth slice. This is a mean as areas where the different structures are difficult to distinguish usually need more pre-segmented slices. Initially, a “limit” label was created delimiting imprecisely all the mouthparts needed (i.e. left mandible without palp and whole maxilliped with both palps). Two tools were used to create the respective “mandible” and “maxilliped” labels. When the image contrast, quality and interlocking of the body parts allowed it, the magic-wand-tool was used which selects all connected voxels with grey values in a range defined by the user. Conversely, the selection was done manually using the brush-tool which allows the user to paint/select voxels. The labels file as well as the RAW file were then saved as Amira mesh (AM) and uploaded into Biomedisa. Biomedisa (Lösel et al., 2020) is an open-source, online segmentation platform developed by different German laboratories. It utilizes the whole 3D image information and an adaptive

random walk approach unlike other traditional interpolation methods who use the labels but not the underlying image data (Lösel et al., 2020). The resulting label file contained the whole segmented mouth pieces.

Missing parts or unsuccessful differentiation of connected structures with similar densities were corrected manually using Avizo. The final volume was generally increased with the volume-grow-tool to close tiny holes in bad quality scans and segmentations. Labels were then selected, resampled keeping only one of two voxels in all axes and eventually compactified when generating the surface. The resulting surface was exported as PLY format (ascii 1.0). Further surface corrections like smoothing, closing of holes, and clean separation of structures was then further done in *Geomagic Wrap* (2013, 3D Systems, Morrisville, U.S.A.). *Meshlab* was used for the creation of mirror images. These were necessary when left structures were damaged or too noisy. Thus, right structures were used in those cases, assuming bilateral symmetry.

Due to the poor quality of the scan, *E. echinata* sp. 1 had only its mandible segmented and not the maxilliped. Therefore, mandible shape data are available for 50 specimens and maxilliped shape data only for 49.

2.5 Geometric morphometrics

Geometric morphometrics is the study of shape variation based on the Cartesian coordinates of anatomical landmarks (Adams et al., 2013; Zelditch et al., 2012). It is based on Kendall's (1977) definition of shape which states that shape is "[the] information that remains when location, scale and rotational effects are filtered out from an object". Using the coordinates of different landmarks on an object allows to have the information of position. Size measurements can also be reconstructed and it is easy to illustrate the results and visualize the relative changes in shape (Zelditch et al., 2012).

2.5.1 Landmarks & semilandmarks

According to the definition of Zelditch et al. (2012), landmarks are "discrete anatomical loci that can be recognized as the same point in all specimens in the study". Ideally, they are *(i)* homologous, *(ii)* provide comprehensive coverage of the object, and *(iii)* are reliable and easy to find. The use of semilandmarks has been developed to visualize curves approximating them with a finite number of points that are therefore neither homologous nor discrete (Zelditch et al., 2012). To superimpose among organism (see below), an algorithm slides them along the tangent to the curve and the shape difference recorded will be the perpendicular displacement to the tangent, *i.e.* the bowing of the curve (Zelditch et al., 2012). It is important to note that

landmarks and semilandmarks are not interpreted individually: individual landmarks do not correspond to "traits" and they only serve to delimit where changes occur; the shape information is contained in the configuration of all the points (Zelditch et al., 2012). What is measured is the configuration of landmarks and it is the response of the whole configuration to some factor that has biological meaning (Zelditch et al., 2012).

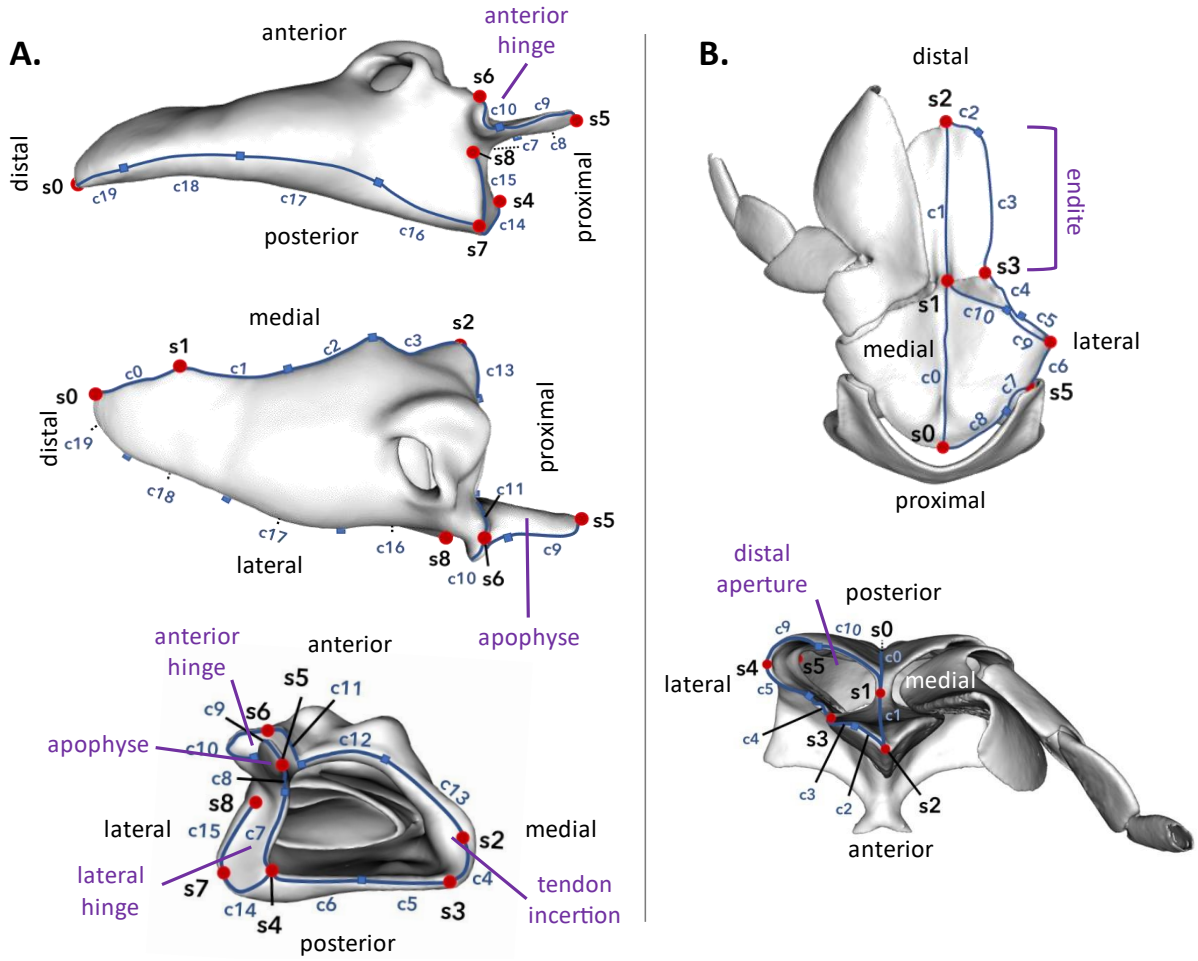

***Figure 7*:** Landmark (red dots) and semilandmarks (blue curves) position on the left mandible (A, lateral, anterior and proximal views) and the left maxilliped basis (B, posterior and distal view). blue dots indicate separation between two curves.

PLY files were imported into Landmark Editor (version 3, IDAV, Davis, U.S.A.). To capture the morphology of the mandibles, a total of 209 points where positioned, 9 landmarks (s0 – s8) and 20 curves (c0 – c19) with 10 points each (*Fig.* 6): s0, most distal tip of the incisor, connected by c0 to s1, the proximal end of the incisor. Along the medial edge, passing over the molar process, curves c1, c2 and c3 connect s1 to s2, a depression along the medial proximal margin where the tendon insertion is. Then, landmarks and curves follow the proximal mandible aperture margin clockwise. S2, over c4, connects to s3, a slight elevation of the border in the medio-posterior corner of the aperture. This connects over two curves, c5 and c6, to s4, the

latero-posterior corner of the aperture margin. From here, two curves, c7 and c8, connect to s5 on the tip of the mandible apophyse following the aperture margin. Two more curves, c9 and c10, follow the anterior apophyse edge and the anterior hinge to connect to s6 in a small depression. From here, c11 connects back to the proximal aperture margin, were c12 and c13 connect back to s2. C14 starts at s4 and connects over the posterior margin to s7. S7 is connected over c15 to s8, meant to capture the shape of the lateral hinge. From s7, four more curves, c16, c17, c18 and c19, follow the lateral edge of the mandible body to reconnect to s0.

The morphology of the inner plate of the maxilliped was recorded using 116 points, 6 landmarks (s0 – s5) and 10 curves (c0 – c10) with ten points each (*Fig.* 6): S0 is at the proximal tip of the basis and follows, via c0, the medial margin until s1, the medial minimum of the curve of the distal aperture. C1 connects s1 to s2 at the distal tip of the endite following still the medial margin. Here, to capture the shape of the inner plate, c2 and c3 follow the outer margin of the endite until s3 were the endite connects with the distal aperture. C4 and c5 connect then to s4, the lateral tip of the distal aperture. From here, c6 connects to s5, the lateral tip of the proximal aperture, from which c7 and c8 lead back to s0, following the proximo-posterior margin of the proximal aperture. From s4 two more curves, c9 and c10, extend following the posterior margin of the distal aperture to reach s1. The configuration matrix was then exported in PTS format for each amphipod mandible and maxilliped.

2.6 Statistical analysis

The statistical analyses were done using R (version 4.0.2), Rstudio (version 1.4.1103) and the packages: *ape*, *geomorph*, *geiger*, *Morpho*, *mvMORPH* and *tidyverse*. Analyses were done independently on mandible and maxilliped shape data.

1.1.1 Generalized Procrustes analysis (GPA)

GPA is an iterative method that minimizes the difference between landmark configurations without altering shape based on Kendall's shape definition (Zelditch et al., 2012). This is done by first translating the centre of the configuration, the centroid, to the origin, then scaling each configuration to unit centroid size which is the square root of the sum of squares of the landmark-centroid distances (Zelditch et al., 2012). Then a configuration is chosen as reference and the second configuration is rotated as to minimize the summed square distances between homologous landmarks (Zelditch et al., 2012). Once all shapes are aligned with the first reference configuration, the mean configuration is calculated and used as new reference for the rotations, which are recalculated (Zelditch et al., 2012). This iterative process stops when the new reference is identical to the previous reference (Zelditch et al., 2012). Here we use the

function *gpagen {geomorph}* to perform the GPA on 3D landmark and semilandmark data using the Procrustes distances to slide the semilandmarks along their tangent directions (Adams and Otárola-Castillo, 2013).

2.6.1 Allometry-free shapes

As stated in the definition of shape, size (*i.e.* scale) is geometrically and statistically independent of shape. However, shape and size can often covary, which is called allometry (Zelditch et al., 2012). The presence of allometry in our dataset was tested using the function *procD.lm {geomorph}* which quantifies the relative amount of shape variation that can be attributed to one or more factors (here, size) in a linear model. The probability of this variation ("significance") is estimated against a null model via distributions generated from resampling permutations (Adams and Otárola-Castillo, 2013). Here we used the linear model formula "Procrustes coordinates ~ centroid size", with 999 iterations. It showed that size explains significant part of the variation for mandibles and maxillipeds ($p < 0.001$). Therefore, to retain only shape information unaffected by changes in size, we created allometry-free shapes, *i.e.* with size-adjusted residuals. The residuals of our linear model were added to the mean configuration (consensus shape) obtained during the GPA to recreate each allometry-free shape. Without this procedure, the first principal components would have mainly represented variation explained by size differences (Mitteroecker et al., 2004).

2.6.2 Phylomorphospace analysis (PA)

To visualize the phylogenetic tree into our morphospace, a PA was performed with the function *gm.prcomp {geomorph}* (Adams and Otárola-Castillo, 2013; Collyer and Adams, 2021; Sidlauskas, 2008). PA is a Principal Component Analysis (PCA) performed on a covariance matrix from species morphometric data estimated using ordinary least squares (Collyer and Adams, 2021). The phylogeny is then projected into the principal components estimating ancestral states for each node (Collyer and Adams, 2021). These ancestral states are reconstructed via squared change parsimony, assuming that the ancestor represented by a node in the phylogeny had an intermediate morphology to the nodes connected to it (Sidlauskas, 2008).

2.6.3 Phylogenetic signal

Phylogenetic signal is the tendency of closely related species to display similar traits due to their common ancestry (Adams, 2014; Blomberg et al., 2003). To measure this, we use Adam's (2014), multivariate version of the Blomberg's *K* statistic which estimates the strength of the signal compared to what would be expected under BM (Adams, 2014; Blomberg et al., 2003).

It ranges from 0 → ∞, where 1 is the value expected under Brownian motion, values of $K < 1$ describe data with less phylogenetic signal than expected and $K > 1$ describes more phylogenetic signal than expected (Adams, 2014; Blomberg et al., 2003). The significance of the K statistic is evaluated by comparing it to the values obtained after tree tips' permutations (Blomberg et al., 2003). *K* and its significance were calculated using the function *physignal {geomorph}* with 1000 permutations.

2.6.4 Modelling trait evolution

Brownian motion (BM) is a stochastic process whose diffusion process can be defined by the following stochastic differential equation: $dX(t) = \sigma\, dB(t)$ where $dX(t)$, the infinitesimal change in a quantitative character X at time t, equals σ, the standard deviation of the BM process, *i.e.* the intensity of the random fluctuation, times $dB(t)$, the "white noise" which, is simply put, represents the stochasticity term of the diffusion (Blomberg et al., 2020; Butler and King, 2004). Used as a macroevolutionary model, BM thus supposes that a character state value $B(t)$ is the result of stochastic drift (Butler and King, 2004; Felsenstein, 1985). It has two evolutionary interpretations: *(i)* evolution occurs by random drift, *e.i.* there is no selection, and *(ii)* there is selection in an environment that varies randomly (Blomberg et al., 2020). As the variance of a trait value increases linearly with time v, this does not make much biological sense as it implies that traits have no physical limits and that evolution has no bounds (Blomberg et al., 2020). The Ornstein-Uhlenbeck model (OU), was first introduced in evolutionary biology by Lande (1976) and by Hansen (1997). It is the most simple expression for selection in an evolutionary process (Butler and King, 2004). According to Lande (1976), natural selection and random drift act both on the phenotypic character stabilizing it towards the local maximum in a fitness landscape (Butler and King, 2004). The diffusion process of OU can be defined by the following stochastic differential equation: $dX(t) = \alpha\, [\theta - X(t)]\, dt + \sigma\, dB(t)$ where α, the strength or restraining force of the stabilizing selection, times the difference between θ, the mean of the process at stationarity, *e.i.* the optimum trait value, add to a stochasticity term of diffusion (Blomberg et al., 2020; Butler and King, 2004). The force of the selection varies with the distance between the current trait value $X(t)$ and the optimum θ (Butler and King, 2004). If the optimum itself varies stochastically, then an OU model remains a good approximation even though the phenotypic evolution is not an OU process anymore (Butler and King, 2004). Species diversify when entering a new adaptive zone (*i.e.* ecological opportunity), which represents sets of similar, ecological niches with abundant resources and without competitors (Harmon et al., 2010; Rabosky and Lovette, 2008). At first, the morphological evolution should

be rapid and then starts slowing down once the available ecological niches start to fill out as species diversity rises (Harmon et al., 2010; Rabosky and Lovette, 2008). This is referred to as the "Early Burst "(EB) model (Harmon et al., 2010). EB is thus a model showing increased constraints on evolutionary change which can be modelled by a slowdown in morphological change through time (Harmon et al., 2010). This predicts that younger subclades, that diversify later in the evolutionary history of an organisms will exhibit less variation than older clades (Harmon et al., 2010). The diffusion process of EB can be put as follows: $dX(t) = \sigma e^{\frac{r t}{2}} dB(t)$ where r is the strength of the exponential change.

Here we use the multivariate versions of these three models (Clavel et al., 2015). We use *mvgls {mvMORPH}* to fit linear models to high-dimensional data sets using penalized likelihood (PL), which results in better parameter estimates than maximum likelihood methods when the number of variables is larger than the number of observations (Clavel et al., 2019, 2015). The models were done using the 'RidgeAlt' penalty with 'null matrix' as the target matrix. This is a rotation invariant method (*i.e.* robust to data orientation and thus the arbitrary choice of baseline shape orientation) with good statistical properties for traits that coevolve while not being too computationally intensive (Clavel et al., 2019). Model fit was tested using the Generalized Information Criterion (GIC; Konishi and Kitagawa, 1996) using the function *GIC {mvMORPH}*, as recommended for penalized models (Clavel et al., 2019).

2.6.5 2-Blocks Partial Least Square analysis (2B-PLS)

2B-PLS is a method to explore covariation between two or more blocks of variables and test if that covariance exceeds what could be obtained by chance (Zelditch et al., 2012). The covariance is quantified using Escoffier's coefficient, a multivariate extension of the ordinary univariate correlation, ranging from 0 (no covariance) to 1 (complete covariance). The statistical significance is then tested by randomizing the order of the observations (Zelditch et al., 2012). 2B-PLS does not assume independence among one set of variables and both sets are treated as jointly and linearly related to a same cause (Zelditch et al., 2012). We used *phylo.integration {geomorph}* to test the correlation between *(i)* mandible shapes and isotopic data, *(ii)* maxilliped shapes and isotopic data and *(iii)* mandible shapes and maxilliped shapes (Adams and Otárola-Castillo, 2013). This function accounts for the phylogenetic relations calculating a covariance matrix under a BM model (Adams and Felice, 2014). The size-adjusted morphological dataset was reduced, and the phylogenetic tree was pruned to the species for which isotopic data were available.

2.6.6 Penalized Multivariate Analysis of Variance (PL-MANOVA)

MANOVA is the multivariate version of the ANOVA test and used here to test whether or not different predictors explain the variance of the response variables significantly. Using *mvgls {mvMORPH}*, the linear model was fitted to our morphometric and stable isotope data: Shape ~ $\delta^{13}C + \delta^{15}N + \delta^{13}C * \delta^{15}N$, shape data explained by isotopic data for C, N and their interaction. Given the use of high dimensional morphometric data, penalized likelihood is used again as the optimizing function. Due to specificities of the function *manova.gls {mvMORPH}*, the 'RidgeArch' penalty was used. The phylogenetic correlation matrix is computed using the best evolutionary model obtained during the model fit (in both cases OU). The significance of each model parameter was then tested using the function *manova.gls {mvMORPH}* which allows to do multivariate tests on generalized least squares linear models fit by penalized likelihood (Clavel et al., 2015). Wilk's test was used with 1000 permutations to create the null distribution. Only the species for which isotopic data was available were kept in the size-adjusted morphological data and the phylogenetic tree.

2.6.7 Disparity through time (DTT)

DTT is used to study the morphological disparity over time. Disparity is measured as the average pairwise Euclidian distance between species, to estimate their dispersion in a multivariate morphological space (Harmon et al., 2003). At each point in time, the disparity is calculated for the whole phylogeny and then for each subclade present at that time. Relative disparities for each subclades are standardized by dividing subclade disparity by the total disparity (Harmon et al., 2003). At each node, the mean relative disparity at that time is calculated as the mean of the relative disparities of all subclades present (Harmon et al., 2003). A DTT plot was created using the *dtt {geiger}* function, our phylogenetic tree and mandible and maxilliped shape data separately and 1000 simulations to construct a null DTT distribution under BM (Harmon et al., 2003). The overall difference in relative disparity between a clade and what is expected under the null hypothesis, the morphological disparity index (MDI), was calculated too (Harmon et al., 2003).

3 Results

3.1 Molecular phylogeny

The resulting tree is presented in figure 8. The names *Echiniphimedia* clade and clade A were kept as in Verheye (2017): the first includes all species of *Echiniphimedia*, the second includes

all species of *Gnathiphimedia barnardi*, *G. sexdentata*, *G. watlingi*, *Iphimediella ruffoi*, *I.*

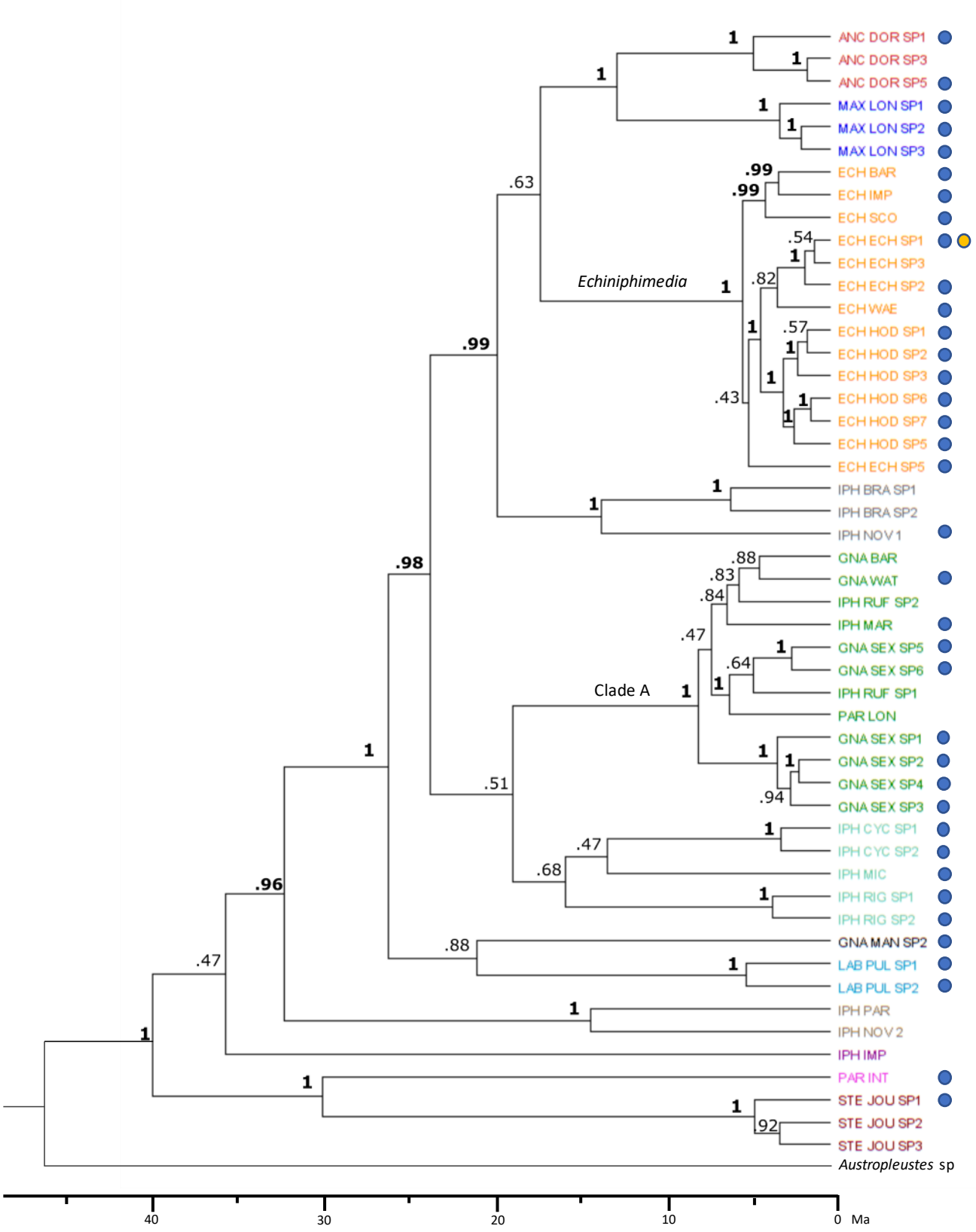

Figure 8 **:** Ultrametric tree of the species from the Antarctic clade of the family Iphimediidae used in this study. Tree based on COI, 28S and H3 genes from Verheye (2017). Outgroup is *Austropleutes sp.* (Pleustidae). Posterior probabilities are indicated on the nodes. Blue dots indicate which species have stable isotope data. Yellow dot indicates that the species has only data for the mandible morphology and not the maxilliped.

margueritei and *Parapanoploea longirostris*.

3.2 Stable Isotopes

Stable isotope data are presented in figure 9 and Supplementary table 1. Highest $\delta^{13}C$ values are found in *Pariphimedia integricauda* (-16.9 ‰) and *Stegopanoploea joubini* sp1 (-17.03 ‰) and the lowest in *G. sexdentata* sp5 (-24.86 ‰) and *L. pulchridentata* (-24,32 ‰). For $\delta^{15}N$, highest values are found in *A. dorsalis* sp5 (16.84 ‰) and *M. longipes* sp2 (15.94 ‰) while the lowest values are found in *G. sexdentata* sp6 (6.55 ‰) and *G. watlingi* (6.98 ‰). *A. dorsalis* and *M. longipes* show generally high values of $\delta^{13}C$ and $\delta^{15}N$ and the species from clade A generally lower values of $\delta^{15}N$ with a high diversity of $\delta^{13}C$. Let's highlight the wide range of $\delta^{15}N$ and $\delta^{13}C$ values found in the *Echiniphimedia* clade and notably for the *E. hodgsoni* complex.

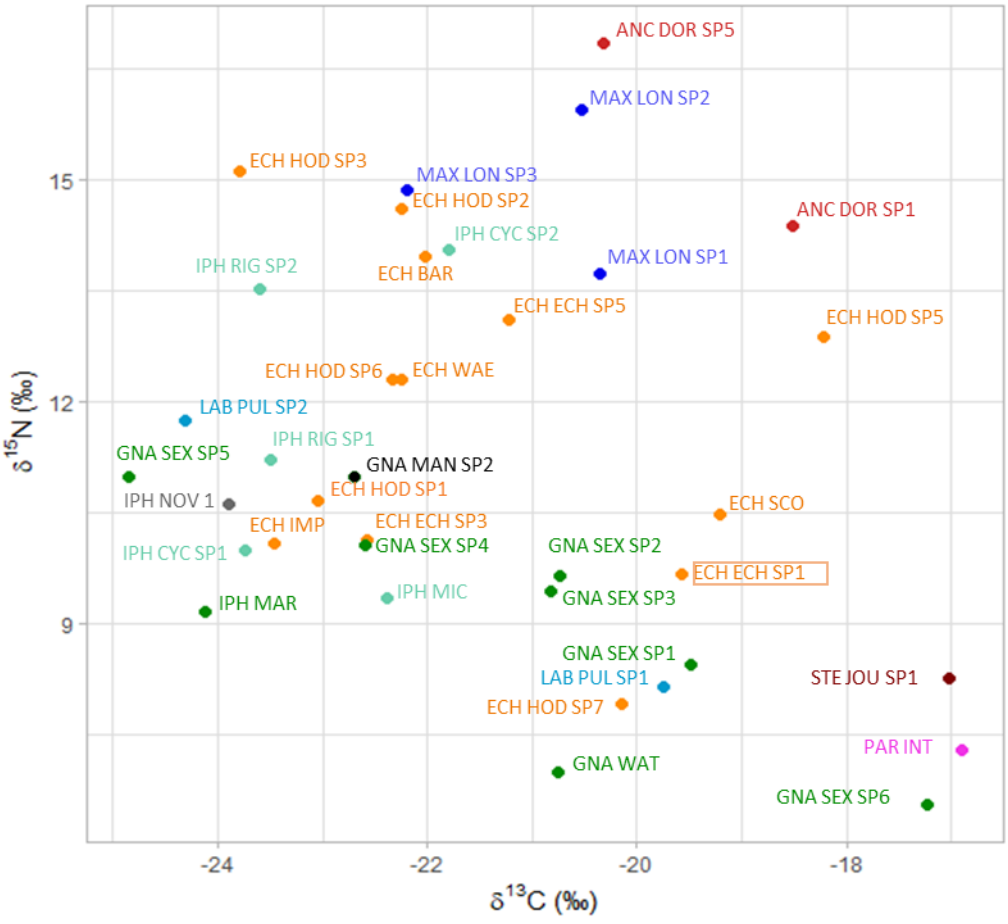

Figure 9 : Carbon and nitrogen isotopic ratios for 37 species of Antarctic Iphimediidae. Colours are according to the ultrametric tree of figure 7. Orange frame indicates that the species has only data for the mandible morphology and not the maxilliped.

3.3 Phylomorphospace

3.3.1 Mandible

For the first three morphospace axes (PCs), the variation explained is respectively 27.13 %, 24.57 % and 9.11 % (60.81 % together). Species-wise, PC1 separates mainly clade A and *G. mandibularis* sp. 2 from all other species. More precisely, we see the *Gnathiphimedia* species, which present very stout mandibles with rounded incisors at the maximum of PC1 together with *I. ruffoi*. Only two species from clade A depart strongly from this general morphology: *I. margueritei* and *P. longirostris*. Most other species — which have a more elongated mandible and an incisor with a cutting edge —are aligned towards the negative side of the axis. PC1 explains the change from a shape slightly narrower and more elongated than the mean shape with a convex mandibular body, a cutting (not rounded) incisor edge, a tiny molar and a narrow and pointy apophyse to a very stout mandible with a straight mandibular body, a curved and rounded incisor, a broad molar and a broad, distally tapered apophyse. Along PC2, species are more dispersed, ranging from *P. longirostris* – with a very thin, long and slightly concave mandibular body, with a relatively short incisor edge and a prominent molar – in the most negative values over a major central cluster with several clades overlapping to *M. longipes* – with a very broad and short mandibular body, a very long, broad and convex incisor edge and practically non-existent molar – in the higher values. PC2 explains mainly change from a pointy mandible shape, very narrow, rather flat and more elongated, with a rather short incisor and a prominent molar, to a very broad mandible with a very convex incisor with a wide edge, and a small molar. The species distribution along PC3 is very similar to PC2 in its species succession except for the presence of *M. longipes* in the lowest values together with *P. longirostris* and the higher values are occupied by *Echiniphimedia*. PC3 shows variation from short and pointy antero-proximal process, strongly depressed tendon insertion surface and broadly expanded lateral hinge in *M. longipes* and *P. longirostris* to a long and broad-ended antero-proximal process, flat tendon insertion and less expanded lateral hinge in e.g. *Echiniphimedia*.

3.3.2 Maxilliped basis

The variation explained by the first three PCs is respectively 40.30 %, 12.05 % and 9.37 % (61.72 % together). The species distribution along PC1 is very distinct as most species cluster around the origin, with *I. rigida* – which has a rather long and straight basis with a rather narrow distal opening and a long endite with a notched tip and slightly rounded lateral margin – having the most negative values and all three *M. longipes* – with a short, broad and rounded basis with a very large and laterally expanded distal opening and a distally tapered shorter endite with a

more rounded lateral margin – positionned far away from all other species in morphospace, at the positive end of the axis. Thus, the main difference explained by the first PC is the size of the distal aperture relative to the length of the inner plate, increasing along the axis. Species-wise, in PC2 we observe *S. joubini*, *P. integricauda* in the lower values, followed by a cluster of most remaining species except for the *Echiniphimedia* clade which is distributed at the positive end of PC2. The basis of *S. joubini* is long and rhomboid with a pointy proximal tip and the narrow distal aperture having its lateral end far posterior to the median end. The endite is thin with a slightly rounded margin and the distal end has pointy tips, the lateral one being larger. *E. echinata* sp5, the most positive species on the axis, presents a triangular, shorter basis with a rounded proximal tip. The distal aperture and the endite are broad and the latter has a relatively tapered/rounded distal end with a more rounded/ laterally expanded lateral margin. Thus, PC2 seems to mainly distinguish along the shape of the basis. For PC3, we find a large cluster of species around the origin with species like *Iphimediella* sp nov. 1 or *I. bransfieldi* in the most negative values and in the most positive values *A. dorsalis* sp. 1, sp. 3 and *Iphimedia*

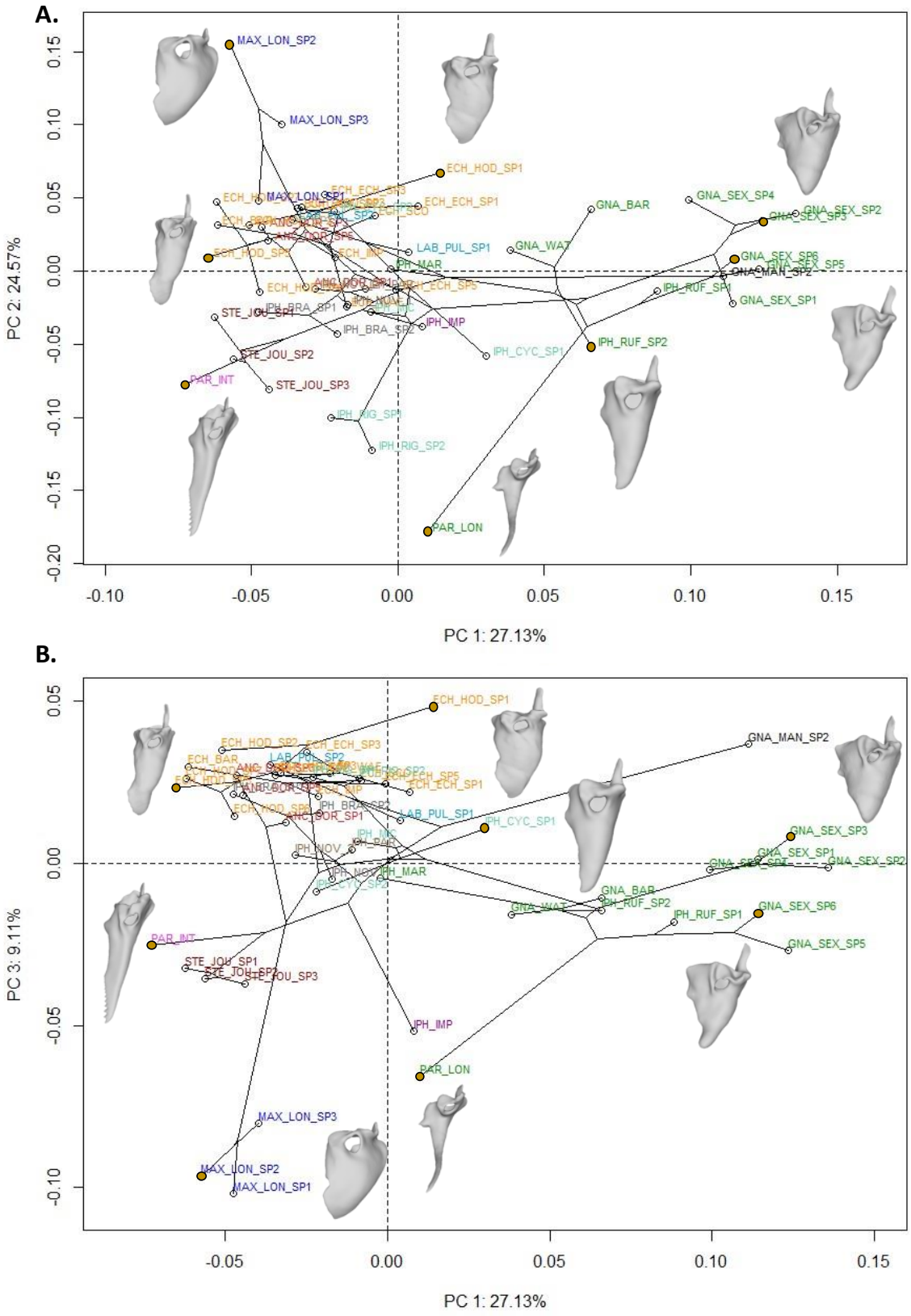

Figure 10 : *Phylomorphospace for mandibles. A. PC1 and PC2. B. PC1 and PC3. Colour code as in figure 7.* Mandibles represented belong to the species with the closest yellow tip.

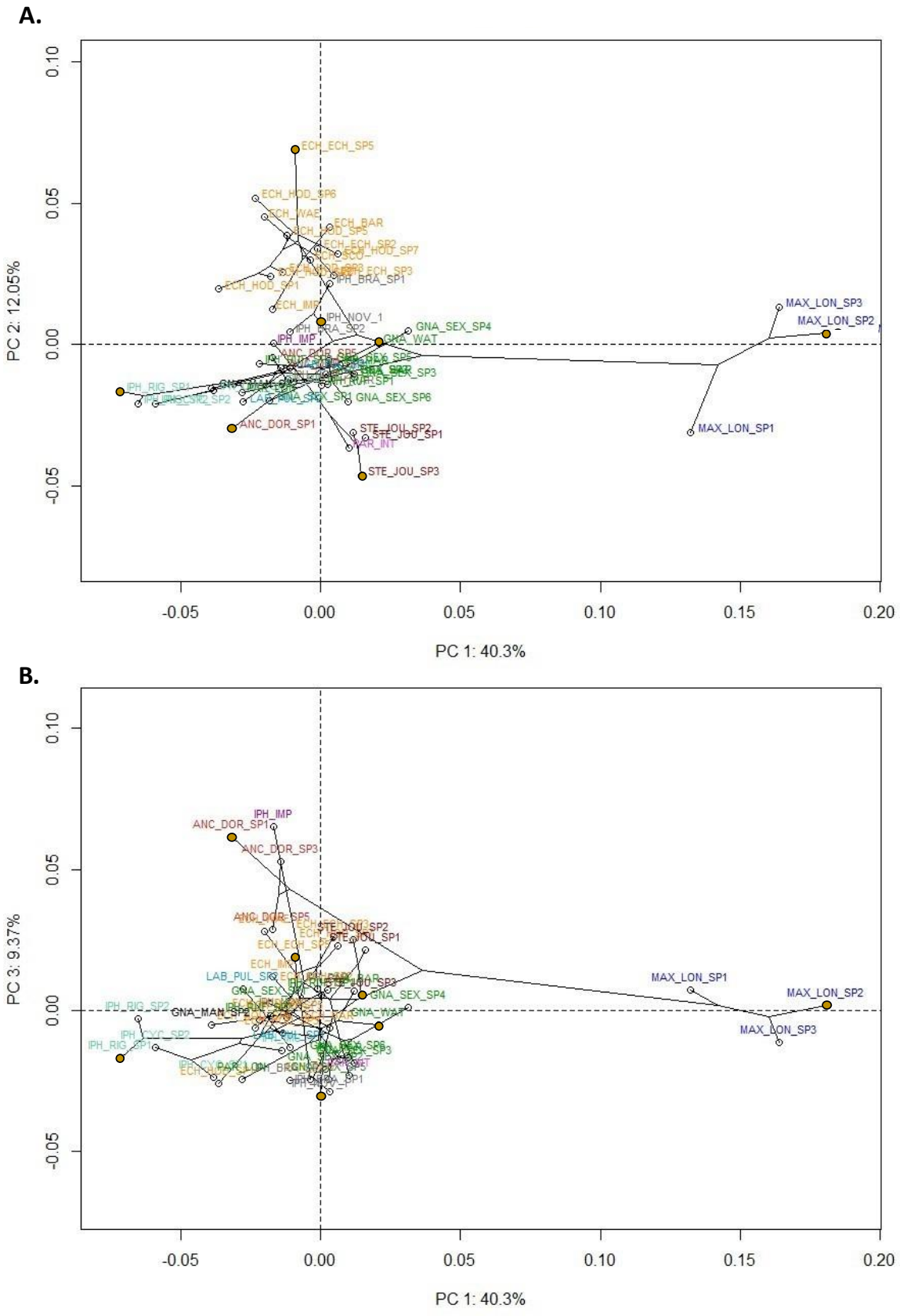

Figure 11 : *Phylomorphospace for the maxilliped basis. A. PC1 and PC2. B. PC1 and PC3. Colour code as in figure 7.* Maxillipeds represented belong to the species with the closest yellow tip.

imparilabia. *Iphimediella* sp nov. 1 has a flat basis with a more rounded proximal tip, a smaller distal aperture and a bit broader endite with a notched distal end, the lateral lobe being larger and higher than the small median one. *A. dorsalis* sp1, on the other side, has a more rounded basis with a pointy proximal tip, a broader distal aperture and the distal end of the endite is rather rounded with laterally lower marginPC3 seems thereby to mainly describe the change in shape of the proximal end of the basis and the distal end of the endite.

3.4 Phylogenetic signal

For the mandible shapes we obtain $K = 0.31$ and p-value = 0.001. For the maxilliped shapes we obtain $K = 0.33$ and p-value = 0.001.

3.5 Trait evolution models

GIC results are presented in table 1. For mandibles and maxillipeds we find that OU is the best suited model with GIC values about one tenth higher than BM and EB in both cases. The strength of the stabilizing selection, α, was estimated. For mandibles $\alpha = 0.737$ and for the maxillipeds' basis we obtain $\alpha = 0.5326$.

Table 1 : Trait evolution models results.

Variable	Model	GIC	Parameters
Mandible	BM	- 295410.3	-
	OU	- 323153.6	α = 0.737
	EB	- 295408.3	r = 0
Maxilliped	BM	- 165787.2	-
	OU	- 178038.4	α = 0.5326
	EB	- 165785.2	r = 0

3.6 2 Block-PLS

Two block PLS results are summarized in table 2. Plots are partly presented in figure 12. P-values underneath 0.05 where only obtained when testing correlation between mandible shape and $\delta^{13}C$ (p-value = 0.024) and when testing between mandible shape and maxilliped shape (p-value = 0.024). Nevertheless, let's note that there seems to be a tendency when testing correlation between maxillipeds and $\delta^{15}N$ data (p-value = 0.076).

Table 2 : 2 Block-PLS results. The green boxes show the p-values lower than 0.05.

Variable 1	Variable 2	R-PLS	P-value
Mandible shape	$\delta^{13}C$	0.678	0.024
	$\delta^{15}N$	0.566	0.271
	0.554	0.374	0.2769
Maxilliped shape	$\delta^{13}C$	0.548	0.398
	$\delta^{15}N$	0.636	0.076
	$\delta^{13}C$ & $\delta^{15}N$	0.607	0.205
Mandible shape	Maxilliped shape	0.812	0.024

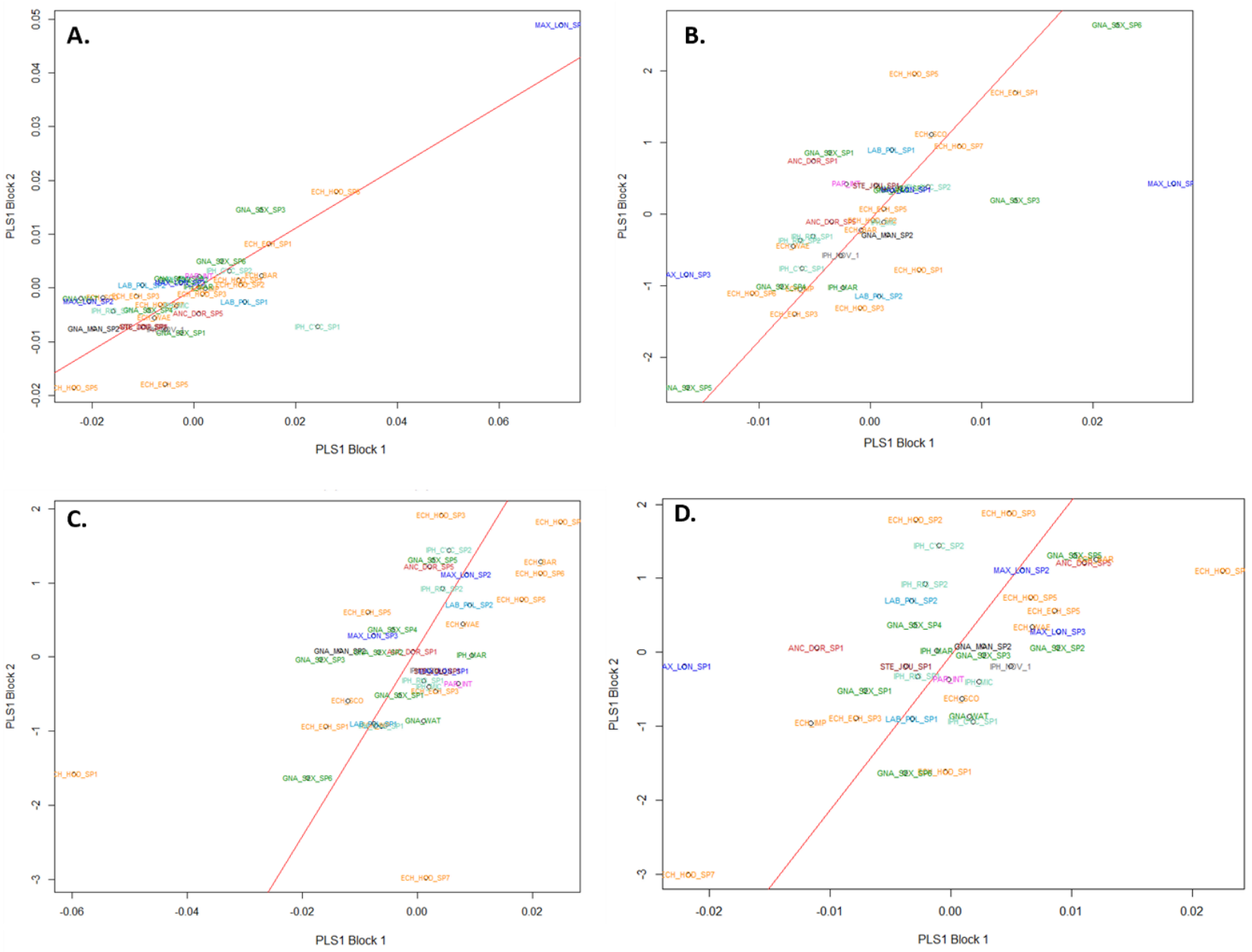

Figure 12 : 2 Block-PLS correlation plots. A. Mandibles vs. Maxillipeds. B. Mandibles vs. δ13C. C. Mandibles vs. δ15N. D. Maxillipeds vs. δ15N.

3.7 PL-MANOVA

For the mandibles the function used an estimated $\alpha = 0.737$. For the maxillipeds $\alpha = 0.2966$. MANOVA results are presented in table 3. For the mandibles no model term explains the variation significantly; the lowest p-value obtained is 0.1698 for $\delta^{15}N$. For the maxillipeds as well, no model term is significant; the lowest p-value obtained is 0.4965 for the interaction $\delta^{13}C*\delta^{15}N$.

Table 3 : PL-MANOVA results

Variable	Model term	Test statistic	P-value
Mandible	$\delta^{13}C$	0.05212	0.2408
	$\delta^{15}N$	0.04683	0.1698
	$\delta^{13}C*\delta^{15}N$	0.6432	0.6174
Maxilliped	$\delta^{13}C$	0.11851	0.5764
	$\delta^{15}N$	0.14277	0.7902
	$\delta^{13}C*\delta^{15}N$	0.09025	0.4965

3.8 Disparity through time

DTT plots are presented in figure 13. For both mouthparts we obtain positive MDIs with 0.131472 for the mandibles and 0.1280832 for the maxilliped basis. Mandibles and maxilliped basis show very similar disparity values over time. Initially, for both, disparity is underneath the median simulated disparity then increase and reach a high at about 24 Ma. Then disparity falls until 19 Ma. Subsequent DTT values are a slightly different. Mandibles' disparity values reach a plateau with some isolated peaks whereas for the

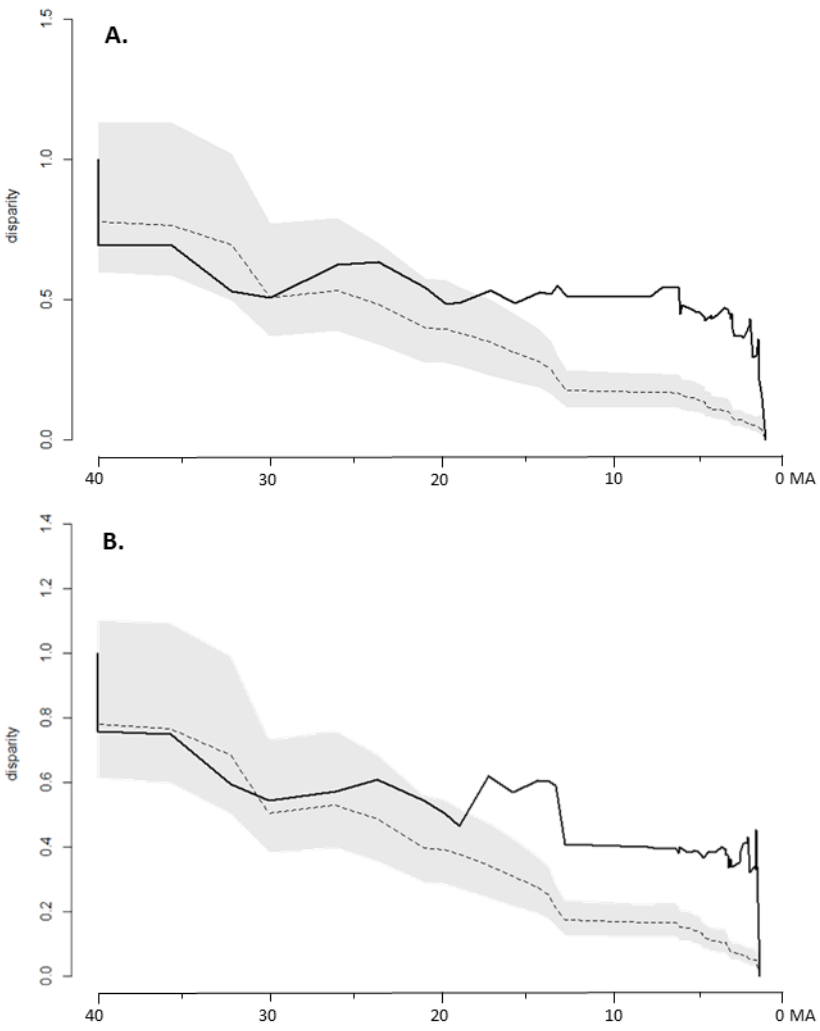

Figure 13 : Disparity through time plots Dottted lines represents the BM null hypothesis median. Shaded area represents the 5% and 95% quantiles for average subclade disparity under the BM null hypothesis. A. Mandible. B. Maxilliped.

maxilliped's basis these small peaks are much more important as disparity reaches a new high at about 17 Ma. This is also when the curves leave the 5% and 95% quantiles for average subclade disparity under the BM null hypothesis. High disparity values are kept until a new low at 12 Ma (still above BM); from then on disparity is constant until it drops to zero close to the end. This is much more abrupt for maxillipeds than mandibles.

4 Discussion

4.1 Morphological diversity of Iphimediidae

Here, using the multivariate version of the Blomberg's *K* statistic, a significant phylogenetic signal was obtained for mandibles and maxillipeds' inner plate. However, $K < 1$ indicates a shortage of statistical dependence among tips compared to that expected under BM (Adams, 2014; Blomberg et al., 2003; Revell et al., 2008). Thus, even if our species present significant resemblance among related species due to common ancestry, the resemblance between two related species is less than that what would be expected if it was proportional to the shared history of the taxa (Blomberg et al., 2003; Revell et al., 2008).

The low phylogenetic signal explains also why PA and regularized phylogenetic PCA (using the OU model) show so little difference. Indeed, when correlation between related species is large, the first PCs will generally show a trend related to the phylogenetic relations among species possibly obscuring other trends in the data (Collyer and Adams, 2021).

With $K = 0.314$ and $K = 0.33$ for mandible and maxilliped's inner plate respectively, the maxillipeds show slightly more phylogenetic signal than the mandibles. Indeed, inner plate shape seems to vary less among closely related species in our PA than mandibles do. Given that the function of the maxilliped probably does not change much among species and is probably not much affected by the food type used, its morphology is more prone to be conserved increasing the phylogenetic signal. Conversely, the mandible shape should have a larger impact on its functionality, thus being more prone to selection and convergence among distant species, eventually lowering *K* values.

Our PA shows that different clades present various degrees of morphological diversity.
The well-supported clade A occupies a large portion of morphospace. They possess an incredibly large distribution specially along PC1 presenting short stout mandibles with rounded tips in the species attributed to *Gnathiphimedia* (except *G. watlingi*), needle-like mandibles of *P. longirostris* whose usage is unknown and more classical shapes with large cutting incisors

in the species formerly attributed to *Iphimediella* (and *G. watlingi*). Both supported subclades in clade A present Gnathiphimedia-type stout mandibles. Remarkably, *G. mandibularis* also converged towards this mandible morphology while being very distantly related. It is actually for the latter that the feeding on Bryozoa has been described (Coleman, 1989b). Thereby, it can be hypothesized that clade A species with similar mandible feed on similar types of hard food sources. Clade A *Gnathiphimedia* show a very wide range of $\delta^{13}C$ values and medium to very low $\delta^{15}N$ values with the two lowest isotopic values of all tested iphimediids. No information was found on SO bryozoan SI values. Nevertheless, bryozoans are one of the most diverse groups in the SO (De Broyer et al., 2014). Not much is known yet bryozoans seem to have different food size preferences (Todini et al., 2018). Thus, one could hypothesize that different bryozoan species feed on different suspended particles or show metabolic diversity leading to different $\delta^{13}C$ values. Thereby, different Iphimediidae with *Gnathiphimedia*-type mandibles could have specialized on feeding on different bryozoan taxa. Of course, such mandibles could be used to feed on other hard prey items like echinoderms as ophiuroid ossicles were found in one individual of *G. mandibularis*. Many ophiuroids are indeed filter feeders thus would not necessarily present high $\delta^{15}N$ values (Byrne and O'Hara, 2017). The very low $\delta^{15}N$ values of *G. sexdentata* sp6 and *G. watlingi* are however difficult to explain as these resemble values expected for a primary consumer. *G. sexdentata* sp6 possesses high $\delta^{13}C$ values that have been suggested to be linked to the consumption of sympagic algae, microphytobenthos and diatoms and *G. watlingi* presents relatively low $\delta^{13}C$ values that could be associated with macroalgae (Aumack et al., 2017; Gillies et al., 2012; Michel et al., 2019; Pasotti et al., 2015). However, the first has rounded and stout mandibles made for crushing rather than cutting, the second has indeed mandibles that can cut but both lack grinding molars and were sampled at over 200 m depth making the consumption of photosynthesising primary producers difficult (Jerosch et al., 2019). This trophic position could instead reflect feeding on sediment particulate organic matter and/or benthic biofilm (Gillies et al., 2012; Michel et al., 2019). The right setation could indeed be enough to support this type of feeding specially for *G. watlingi* as *A. dorsalis* has a similar type of mandible and is a documented detritus feeder (Coleman, 1991; Dauby et al., 2001). Being able to observe the setation or lm could perhaps help elucidate this in addition to the classical studies of gut content or fatty acids.

As stated above, *P. longirostris* is an outstanding species with a unique needle-like mandible morphology that marks the incredible morphological diversity of clade A and for which one expects a very specialized feeding strategy. Like for most amphipods, no literature on this species was found except for morphological descriptions. SI values obtained for three

individuals from Adelie Land not used in this study show $\delta^{13}C$ about -22 ‰ and $\delta^{15}N$ about 9.7 ‰ which suggests rather omnivory. It could be hypothesized that the dentated short incisor at the end of the curved needle-like mandible and which protrudes from the conical mouthpart bundle could be used to be inserted in tight spaces and cut soft tissues protected inside like bryozoa or capture polyps on anthozoans. Styliform mandible and maxilla have been suggested to help pierce and push the mouthparts into the tissue of the sea-anemones on which it feeds sucking up the tissues(Coleman, 1991; Dahl, 1964).

The *Echiniphimedia* clade is more clustered in comparison to clade A. Nevertheless, visual examination suggests that this is not necessarily because clade A changed morphologically more than the former (*i.e.* unequal magnitude of diversification) but could be explained by how the morphological differences distribute through the morphospace (*i.e.* unequal mode of diversification; Sidlauskas, 2008). After their separation, *Echiniphimedia* continued to speciate and diversify morphologically but within a narrower range of morphological possibilities leading to the convergence in distant species like *E. barnardi* and *E. hodgsoni* sp7. Most *Echiniphimedia* species present high $\delta^{15}N$ values. Yet, information on feeding ecology is missing for most species in this clade and it can only be stated that at least one species of the *E. hodgsoni* species complex is presumably a sponge micropredator (Coleman, 1989a; Nyssen et al., 2002; Verheye, 2017). Nyssen et al. (2005) measured highest intraspecific variability in *E. hodgsoni* with values varying between 10.6 ± 1.8 ‰ for $\delta^{15}N$ and –24.3 ± 1.3 ‰ for $\delta^{13}C$. Even so, our $\delta^{15}N$ and $\delta^{13}C$ values for *E. hodgsoni* differ and only sp1 and sp6 fall in the interval he presentes. This variability might be due to individual differences between organisms or, likely, to the confounding of different species inside the same complex. The high variability in $\delta^{13}C$ in the *Echiniphimedia* clade could indicate high variability in their food sources. Notably, for *E. hodgsoni* this could suggest that the different species feed on different species of sponges, that they complement this sponge diets with different other food sources or, also, that they possess completely different food sources. Existing isotopic data for different sponge species in the Antarctic shows indeed large variation in $\delta^{13}C$ and $\delta^{15}N$ values between species and between sampling stations which would fit with our results. Thurber (2007) measured $\delta^{15}N$ values for sponges ranging from about 4.5 ‰ to about 11.5 ‰ and $\delta^{13}C$ values ranging from about -23.8 ‰ to about -21.5 ‰ in the Ross Sea. Michel et al. (2019) measured values $\delta^{15}N$ values for sponges ranging from about 6.5 ‰ to about 13 ‰ and $\delta^{13}C$ ranging from about -21 ‰ to about -17.3 ‰ in Adelie Land. Notably, both authors obtain substantially different values for the species *Homaxinella balfourensis*. Thurber (2007) also observed differences between

same species individuals from different depths. Both these studies remind us of the impact that different sampling location and time (and possibly species identification) can have on isotopic data. Like for clade A, we see that there is high morphological convergence between *E. barnardi* and *E. hodgsoni* sp7, yet both present very distinct isotopic values. Thus, here too one can suspect that the same mandible type is used in different feeding strategies.

This correlation towards a *Echiniphimedia* type mandible morphology seems to generally apply to most Antarctic Iphimediidae. Indeed, *Anchiphimedia*, *Labriphimedia* and species like *I. paracuticoxa* and *I. bransfieldi* cluster together with *Echiniphimedia* in mandible morphospace. This corroborates our low phylogenetic signal insisting on the low morphological correlation among closely related species and the morphological convergence of distant species. This *Echiniphimedia* type has a medium long, straight body, medium broad with sharp incisor edge cutting in the frontal plane, with a reduced mandible and big enough antero-proximal process and tendon insertion point as to attach sufficient muscles and thus be able to apply sufficient force to cut through different prey items. This morphology seems adapted to a large range of trophic niches from sponge browsing in the *E. hodgsoni* complex to detritus feeding in *A. dorsalis* and macropredatory feeding as suggested from gut content and/or isotopic data for some *Iphimediella* and *L. pulchridentata*. This mandible morphology probably allows some extent of opportunistic feeding that has been suggested to be important in the SO and in Iphimediidae at least *Iphimediella* as they do not feed exclusively on one single prey item (Dauby et al., 2001; Michel et al., 2020, 2019; Nyssen et al., 2005).

The high $\delta^{15}N$ values we observe in our data for *A. dorsalis* correspond well with the detrital feeding habit inferred from gut-content (Coleman, 1991). Detritus feeders often present high $\delta^{15}N$ values as they feed on decaying matter often already passed through microbial loops that enrich the organic matter in heavy ^{15}N isotopes (Michel et al., 2019; Nyssen et al., 2002). Yet, we observe about 2.5 ‰ difference in $\delta^{15}N$ values between *A. dorsalis* sp1 and sp5. Even morphologically this two species lye rather far away in morphospace: sp5, like sp3, is stouter with a broader more protruding incisor edge, sp1 is pointier, straighter with a shorter incisor and more like Coleman's (1991) plates. This could suggest that this individual fed on some carrion of a species high in the food web, however, other scavengers do not show that high $\delta^{15}N$ values in Nyssen et al. (2002). An environment with a stronger microbial loop could also lead to increased organic matter in the sediment (Nyssen et al., 2002).

In *L. pulchridentata* both individuals show different morphologies as well as different isotopic values. Sp1 has a straight mandible with a short incisor while sp2 is very similar to

Echiniphimedia type thus broader and with a large slightly curved incisor edge. As sp2 shows 3.5 ‰ higher $\delta^{15}N$ values than sp1 on could suggest that it is a predator perhaps even feeding on sponges like *Echiniphimedia hodgsoni*, and sp1 might be an omnivore.

For *I. cyclogena,* SI values observed by Nyssen et al. (2002) do not correspond well: we observe nearly 4 ‰ higher $\delta^{15}N$ values in sp2 than sp1 and while *I. cyclogena* sp1 is very close but below values, *I. cyclogena* sp2 presents far higher values for both isotopic ratios. High $\delta^{15}N$ values for *I. cyclogena* are also relatively in line with what is known from their feeding behaviour. A wide range of $\delta^{15}N$ and $\delta^{13}C$ values were found for Holothuroidea by Nyssen et al. (2002) which are the alleged food sources on which this amphipod species are presumably specialized (Dauby et al., 2001). As he measured $\delta^{15}N$ values up to 12 ‰ this could indeed still explain the high values of sp2. Moreover, there is a 250 m depth difference between both sampling stations which could also account for some difference (Thurber, 2007). However, as the species inside the complex differ in SI values and morphology one could suggest that feeding strategy differs too. Indeed, sp2 seems more like the *Echiniphimedia* type and might rely more on high $\delta^{15}N$ resources like sponges or carrion. While Michel et al. (2020) describes a dentate incisor we do not observe this here possibly due to the quality of the scans and cannot comment on differences on this regard.

M. *longipes* shows a very specialized mandible morphology and sp2 separates strongly from all other Iphimediiae. Here too we observe morphological variation inside the clade along PC2 as sp2 positions itself close to the *Echiniphimedia* type as it is more elongated and sp3 is intermediate. High $\delta^{15}N$ values for *M. longipes* are also relatively in line with an alleged consumption of Anthozoa since a wide range of $\delta^{15}N$ and $\delta^{13}C$ values were found for this group (Coleman, 1989a; Dauby et al., 2001; Nyssen et al., 2002). Like for *I. cyclogena* we have no proof that the different species inside the complex use the same food source as the complex was unknown in previous studies and we do observe differences in isotopic values (Coleman, 1989a; Dauby et al., 2001). Nevertheless, the range in $\delta^{15}N$ values is a bit smaller (about 2 ‰).

The basal *S. joubini – P.integricauda* clade that presents long straight mandibular bodies with a relatively long and thin incisor, strongly dentated in *P. integricauda* (ten cusps) and smooth in *S. joubini* with the tip curved medially, and both with a relatively large molar process. Epiphytic diatoms seem to be the primary food source of *P. integricauda* (Aumack et al., 2017) which is in line with the low $\delta^{15}N$ and high $\delta^{13}C$ values we observe in our specimen and the depth at which it was collected. The strong dentation might help scraping and grasping these diatoms. Yet, our $\delta^{15}N$ and $\delta^{13}C$ values are higher than those observed in Aumack et al. (2017).

As this is not a complex this could just be due to individual variability and a regime more supplemented in crustacean as this resource has also been found in their gut content (Aumack et al., 2017).

As the morphologies and SI values are similar and no feeding habit has been described so far, one could suggest that *S. joubini* could also feed on diatoms. Yet it was collected far deeper (250 m depth) which speaks against the consumption of epiphytic diatoms. Sedimented organic matter could be an option and as its $\delta^{15}N$ values are higher a more omnivorous regime could also be supported.

No Iphimediidae occupies a low $\delta^{13}C$ - low $\delta^{15}N$ niche. This area has been associated with herbivory or suspension feeding as macroalgae and suspend particulate organic matter often present low $\delta^{13}C$ values (Aumack et al., 2017; Gillies et al., 2012; Michel et al., 2019; Nyssen et al., 2005, 2002). Aumack et al., 2017, studied amphipod assemblages in habitats dominated by macroalgae and found that feeding on macroalgae was rare and amphipod species studied were to a large part predominantly primary consumer using epiphytic diatoms and filamentous endo/epiphytic algae as resource along the western Antarctic peninsula. Similarly, to our results, Dauby et al., 2001, observed this absence of herbivory too in his Weddell Sea communities and explained it with the absence of macroalgae in the sampled ice-covered deep shelf environments. Most of our samples come from deeper waters too, where most iphimediids are found, which could explain this phenomenon. Morphologically, herbivory is mainly marked by the presence of proficient grinding molars (Aumack et al., 2017; Dauby et al., 2001; Michel et al., 2020) which are absent in Iphimediidae which only possess fleshy lobes to the most. Let's note that, even if it certainly does not affect our interpretations in any way, our methodology does not allow to visualise this area very well and the tips of the molars were sometimes lacking.

Similarly, adaptations to suspension feeding seems to rely mainly on long and strong setae for filtering the water column which are absent in the studied species which excluds this possibility (Coleman, 2007; Dauby et al., 2001; De Broyer et al., 2001; Michel et al., 2020).

As seen with the phylogenetic signal values, the maxilliped basis morphology present more similarities between closely related species than mandibles do. The basic morphology seems rather strongly conserved while variation occurs mainly on broadness and length of the general structure. As for the mandibles, it seems that subclades continued diversifying leading to branch overlaps and morphological convergence in a restricted morphospace reducing the morphological covariance between closely related species. The most explicit change in morphology is that of *M. longipes* with its very stout basis with a broad distal aperture and short

endite. This difference in maxilliped inner plate morphology is so outstanding that it seems difficult not to expect it to be some type of adaptation to its feeding strategy specially when considering that this species is presumably a very specialized cnidarian feeder which is to our knowledge unique in Iphimediidae (Coleman, 1989a). Coleman, 1989a, suggested that *M. longipes* might ingest larger food particles than *E. hodgsoni* based on foregut structures. One could thus hypothesise that the as the food particles are large, smaller inner plate could allow bigger pieces to enter the preoral cavity and be enough to push food towards the molars. The large and wide distal aperture suggests also large outer plates which are indeed present. No information was found on the inner plate of another amphipod feeding on cnidarians *Stegocephaloides christianiensis* (Stegocephalidae; Moore and Rainbow, 1984), yet Stegocephalidae have apparently rather a well-developed inner plates (Lowry et al., 2003). For the other species of Iphimediidae it is difficult to give a biological explanation to such slight differences in broadness, length and endite tip without a clear understanding of the way in which it is used, the interplay and relative size between different mouthpieces, and the food type consumed by the species. There does seems to be distinctive morphologies for the *Echiniphimedia* clade or the basal *S. joubini – P. integricauda* subclades. In what ways a rounded endite tip could help push sponge parts into the mouth better than an endite with a forked tip seems unclear and how the latter could help for feeding on diatoms too. With our CT scans we are unable to capture the setation of the maxilliped thus, further information is lost on how endite shape could be adapted to the feeding strategy as we cannot consider how shape might be changed to optimise the support and use of setation in different contexts. Shape changes in the distal aperture nevertheless, as we supposed for *M. longipes*, could be due to a more important outer plate. This is observed in *M. longipes* compared to *E. hodgsoni* in Coleman (1898) and visual analysis of the scans during segmentation seem to corroborate this. The outer plate has a wider range of motions than the inner plate does and as it covers the other mouthpieces and can help grasps and hold food its morphology might be more inclined to be selected upon than the inner plate. Thus, it looks like there is a limited space in morphospace where most species can be found: a slender basis with an endite about as long as the rest of the basis and about one and a half times longer than the distal aperture is long. This distal aperture is also generally about double as long as it is broad.

4.2 Ecomorphological adaptation

We here used stable isotope data as a proxy for the trophic niche of our organisms and tested if this trophic niche could explain the morphology of the mandible and the maxilliped's basis under the hypothesis that mandible morphology is adapted to the feeding strategy.

The 2B-PLS "phylogenetically-corrects" our morphological and isotopic data with a BM model, which as we found out is not the best fitting model for our data. Nevertheless, the plots obtained allows us to extract some information on the correlation of both datasets. Indeed, while not significant our plots seem to indicate a rather good correlation among mandible shape and both isotopes together. As the $\delta^{15}N$ plot is very similar to the one with both biomarkers and $\delta^{13}C$ is significantly correlated, it seems that the main reason for the lack in correlation happens due to the $\delta^{15}N$ of some species. Indeed, two species seem to deviate a lot: *E. hodgsoni* sp1 and sp7. The first has a very stout mandible with a very broad incisor edge, the second, conversely, is thinner and longer yet still with a broad incisor. Thus, both still show a rather typical *Echiniphimedia* type mandible but sp1 is closer to the maximum values of PC1. Thereby, it could be that the test expects sp1 to have higher $\delta^{15}N$ values as it comes closer to *M. longipes* instead of the medium values it has and expects sp7 to show medium $\delta^{15}N$ values instead of the very low values that is has. It is difficult to explain these outliers as it could be due to "errors" in the SI values as well as it could be due to special unknown feeding strategies or the large variation in sponge SI values. Conversely, $\delta^{13}C$ is significantly correlated with the mandible morphology. Of course, this can be due to the bias created from using a BM model.

Similarly, for the maxilliped basis there seems to be a tendency towards correlation between its morphology and $\delta^{15}N$, thus possibly correlated to trophic niche. The large morphological difference observed for *M. longipes* sp2 and its high $\delta^{15}N$ values seem to be the best fitting species thus it could be suggested that the correlation implies higher $\delta^{15}N$ values for a shorter basis with a larger distal aperture and thus larger outer plates.

However, the PL-MANOVA based on an OU model, the better fitting evolutionary model for our morphological data, does not give any significant result for neither mandible nor maxilliped inner plate. Thus, the variability in morphology cannot be explained by neither $\delta^{13}C$ $\delta^{15}N$ nor a combination of both. Similar results were observed by Michel et al. 2020, who tried to show correlation between mandibles and feeding habits using nine Antarctic amphipods from seven different families and five functional groups. Mandible morphology was relatively compatible with the known feeding habit of the species yet the links between both were not explicit. Indeed, much like in Iphimediidae, different feeding strategies presented similar adaptations and

different adaptations can be found in the same feeding strategy. Examples would be the *A. dorsalis* complex that are positioned close to the *Echiniphimedia* type mandible in morphospace. The first is allegedly detritus feeders, the second are hypothesized sponge feeders yet both converge towards the same morphology. As Michel et al. (2020) put out, dietary specialization can be linked with marked changes in the morphology of other mouthparts and indeed, *A. dorsalis* present brush-like setation of the maxillae and maxilliped outer plates with a morphology that would speak in favour of this detrital feeding strategy and that are absent in *Echiniphimedia* (Coleman, 1991). Examples for species with the same feeding strategies but that do not share the same morphology are more difficult to give as we lack ecological information for the different species inside the complexes. Nevertheless, *E. hodgsoni* sp6 and *E. waegelei* practically overlap in our SI plot yet are no direct neighbours in morphospace. *E. waegelei* has a stouter mandible and has a longer antero-proximal process. If this does practically a big difference remains to be seen, thing is this certainly affects our statistics.

Our 2B-PLS for correlation between mandible morphology and maxilliped basis morphology is significant. *M. longipes* is certainly to a large part responsible as extreme mandible shape combines to extreme maxilliped inner plate shape. We see *E. hodgsoni* stand out, higher than most *Echiniphimedia*, as its stout mandibles stands out in this clade. Similarly, *I. cyclogena* sp2 is also outstanding and indeed while its mandible cluster close to *Echiniphimedia*, its maxilliped basis does not as it closely relates to that of the other species in its clade.

4.3 Morphological trait evolution

For mandibles and for the basis of the maxilliped we obtained that the preferred model of trait evolution is OU. The OU model indicates a "pull" towards an optimum and thus adaptive evolution (Butler and King, 2004; Uyeda and Harmon, 2014). However, that our data fitted an OU model best means above all that an early burst with subsequent decrease in diversification rates as well as a stochastic model are not supported. The OU model will thereafter be the best suited model in any case where variance of a trait does not grow indefinitely over time and reaches stationarity (Boucher and Démery, 2016). Thus, it could also represent a case with a neutral mode of evolution under hard constraints (bounds set by selection or not) as we did not specifically test for it (Boucher and Démery, 2016). Examples of bound would be for instance an upper limit size due to oxygen availability, niche limits due to competition and predation or limited genetic variation in a lineage that would constraint a character between two extreme values (Boucher and Démery, 2016; Chapelle and Peck, 1999). In both, bounded BM (BBM) and OU, a trait has a limit on the total variance that it can accumulate over time (Boucher and

Démery, 2016). Using an ultrametric tree a Late Burst of diversification would also not be distinguishable from an OU model (Slater et al., 2012).

Our PA seemingly corroborates this finding for both mouthparts studied as our data presents low phylogenetic signal and we observe morphological convergence in distant species. Revell et al. (2008) showed using simulations that a range of evolutionary processes could result in low phylogenetic signal: strong stabilizing selection towards a single optimum, strong regular divergent selection, rare stochastic peak shifts, genetic drift with increasing rates over time, and increasing niche shifts over time which all could be here best fitted by an OU model as it is not BM or EB (Revell et al., 2008). As we have not tested for more elaborate models it is difficult to know exactly what evolutionary process fits best our data.

For mandibles and maxillipeds we observe positive MDI values indicating that the disparity among subclades is above that expected under BM (Harmon et al., 2003). Indeed, as shown above, Iphimediidae clades are highly diversified and present morphological convergences. Our DTT plots start with lower disparity than expected, suggesting more disparity among clades than within, although it does not fall outside the confidence interval of expected disparity under BM. This once again reminds us of the non-significant decrease in lineage diversification rates observed by Verheye (2017). As showed through simulations by Colombo et al. (2015), an EB signal might not be detected if hard or soft boundaries apply and as our α values are about 0.3 and 0.7, this would apply to us. After these negative values, both DTT plots experience a first peak in disparity at the Oligocene - Miocene boundary during a period qualified by Crame, 2018, as a mixed phase of radiation and extinction due to glacial expansion and early Miocene warming. Yet this falls in the confidence interval and should be interpreted cautiously. The second peak (whose presence also speaks rather against an early burst of diversification; Wilson et al., 2013) happens at about 17 Ma, before the MMCO, when the *Echiniphimedia* clade diverges. This is also when our curve leaves the 5% and 95% quantiles for average subclade disparity under the BM null hypothesis. Verheye (2017) observed an increase in speciation rate at the base of *Echiniphimedia* and interpreted a burst of allopatric speciation as a result from repeated isolation of populations in ice-free refugia during glacial maxima. Here we can add that this is associated to an increase in the diversity of morphologies in mandible and maxilliped basis. This is also about the time when the (specially for mandibles) very diversified clade A separates. High disparity and MDI values can result from boundaries to trait evolution or elevated rates of diversification near the present. Indeed, *Echinipihmedia* and clade A diversified about 3.8 MA and 7.8 Ma respectively, after the MMCT, during the late Miocene to

Pliocene (Verheye, 2017). This diversification has been suggested to be due to allopatric speciation events from repeated isolation events in refugia as seen in notothenioid fishes or due to a key innovation leading to a new ecological opportunity (Verheye, 2017). For both, adapted mouthparts might have allowed the colonisation of a new niche: sponges for *Echiniphimedia* and Bryozoa for clade A as suggested by Verheye (2017). In the Antarctic, no other sponge feeding amphipods have been recognized at least to our knowledge (Amsler et al., 2009). For clade A, feeding strategies are unknown but we have hypothesized that, given the morphological convergence, they might be similar to the bryozoan feeding *G. mandibularis*. This key innovation should have allowed to enter the new and vacant niche of bryozoan predation. However, the question remains on why the *G. mandibularis* clade did not have a burst of diversification since nowadays only two putative species are known (Verheye, 2017). As Losos (2010) explains this could be due to quite different reasons like (i) the actual absence of an ecological opportunity with no appropriate niche for the species perhaps already occupied by a species that just radiated (clade A could perhaps already occupy the niche), or (ii) to the inability to speciate or evolve for example due to the incapacity of a certain phenotype aspects to evolve independently or a lack of behavioural or phenotypic plasticity. The latter might also explain why some species evolving key innovations might not radiate like the aardvark. This evolvability seems to be relatively clade specific, some radiate others don't, Warblers radiated on the Galapagos but also on the mainland, yet mockingbirds have neither on the mainland nor on the Galapagos (Losos, 2010). Thus, ecological opportunity could be rather of "heuristic value" as it helps explain when radiation happens but not when it does not (Losos, 2010). Nevertheless, the relationships between clades are still not completely well established and new genes and species might ad new information.

As we do have high disparity among clades with low phylogenetic signal and morphological convergences this does not speak in favour of a single optimum and may reflect rapid divergence. Indeed similar results, with high MDI values and support for an OU model, were obtained in a study of the opercular shapes of icefish by Wilson et al., 2013. As their results presented high dispersal of their species in their PA. They suggested that the high disparity measured in closely related species might conflict with the idea of an optimum and suggest the support for the OU model indicates a loss of phylogenetic signal due to potential rapid divergence rather than a convergence towards an optimum. To explain the overlap in opercle shape between species with different feeding strategies, they hypothesize that this is due to the fact that notothenioids have little competition and thus do not need to strongly adapt their

morphology. Thus, a generalist shape can be kept. This might also apply to our species as we observe a lot of convergence. This potential rapid divergence might be linked to repeated adaptive radiations as it has been observed in notothenioid fishes or damselfishes (Colombo et al., 2015; Frédérich et al., 2013; Rutschmann et al., 2011).

4.4 Limits and perspectives

As stated several times, this study is confronted with a low number of individuals per putative species. This might bias morphological and isotopical results. Especially for studying the trophic ecology using one single individual is very limiting giving the high intraspecific variability that can exist. Moreover, we did not standerdized said isotopic values per station making it difficult to compare individuals. Isotopic values should ideally be used in combination with other methods that can give information on the trophic ecology of a species like gut content, fatty acids composition or *in situ* observation of feeding behaviour. All these are lacking for Iphimediidae or do not take into account species complexes which makes interpretation of our results difficult.

Choice of our landmarks might also be questioned as many are Bookstein's type 2 landmarks, *i.e.* local maxima or minima of curvature. They are more difficult to define and position correctly on different organisms, Zelditch et al., 2012, nevertheless, still encourages their use if one tries to minimize the error when positioning them in each species as they still can give a lot of information. Moreover, *Landmark editor* lacked flexibility when positioning curves and thus might have created some small artefacts. These are mainly seen in the maxilliped basis, especially around the endite whose border was often of pour quality in the scan. While present and ideally avoided they might not really have impacted the overall structure of the basis and thus the morphological analysis.

Thus, perspectives are an error study for landmarks, the use of more individuals per species and possibly additional species, the complementation of trophic niche information with other methods, training of the *Biomedisa AI* to accelerate the segmentation process, the use of another more elaborate software to position landmarks and the development of more elaborated evolutionary models considering more optima and/or model shift at some point during the evolution of Iphimediidae to better understand their evolution. Testing for BBM would be and initial step as well as rate shifts to test if we observe a late burst. Specially SI data and models should be our main target in further developments.

5 Conclusion

Iphimediidae show little but significant phylogenetic signal, presenting high among subclades diversity. For some clades, this is restricted to a reduced area of morphospace, which is due to different modes of morphological diversification rather than differences in magnitude. Our species present high convergence in mouthpart morphologies. For mandibles this might be due to the high versatility of functions that can be done with this mandible type; for the inner plate of the maxilliped this might be due to the conservation of its limited function. As we do not find a relation between trophic ecology and morphology as we are confronted with one-to-many and many-to-one scenarios. As OU is the best models this might mainly be due to a rapid change in diversification as it happened for icefishes. One should retain that we have with certainty no BM nor a EB model but instead adaptive evolution. Morphology that allows for adaptability and opportunistic behaviour seems of interest in such a difficult environment as the Antarctic shelf. The Plio-Pleistocene have certainly affected the modern Iphimediidae probably responsible for the erosion of the signal of former radiations and by likely being responsible for the radiation and the creation of pseudo-cryptic species notably in *Echiniphimedia*, clade A, *A. dorsalis* or *M. longipes* that all present different morphologies.

6 References

Adams, D.C., 2014. A Generalized K Statistic for Estimating Phylogenetic Signal from Shape and Other High-Dimentional Multivariate Data. Systematic Biology 63, 685–697.

Adams, D.C., Felice, R.N., 2014. Assessing Trait Covariation and Morphological Integration on Phylogenies Using Evolutionary Covariance Matrices. PLoS ONE 9, e94335. https://doi.org/10.1371/journal.pone.0094335

Adams, D.C., Otárola-Castillo, E., 2013. geomorph: an R package for the collection and analysis of geometric morphometric shape data. Methods Ecol Evol 4, 393–399. https://doi.org/10.1111/2041-210X.12035

Adams, D.C., Rohlf, F.J., Slice, D.E., 2013. A field comes of age: geometric morphometrics in the 21st century. Hystrix, the Italian Journal of Mammalogy 24. https://doi.org/10.4404/hystrix-24.1-6283

Allcock, A.L., Strugnell, J.M., 2012. Southern Ocean diversity: new paradigms from molecular ecology. Trends in Ecology & Evolution 27, 520–528. https://doi.org/10.1016/j.tree.2012.05.009

Amsler, M.O., Mcclintock, J.B., Amsler, C.D., Angus, R.A., Baker, B.J., 2009. An evaluation of sponge-associated amphipods from the Antarctic Peninsula. Antarctic Science 21, 579–589. https://doi.org/10.1017/S0954102009990356

Aumack, C.F., Lowe, A.T., Amsler, C.D., Amsler, M.O., McClintock, J.B., Baker, B.J., 2017. Gut content, fatty acid, and stable isotope analyses reveal dietary sources of macroalgal-associated amphipods along the western Antarctic Peninsula. Polar Biol 40, 1371–1384. https://doi.org/10.1007/s00300-016-2061-4

Blomberg, S.P., Garland, T., Ives, A.R., 2003. Testing for Phylogenetic Signal in Comparative Data: Behavioral Traits Are More Labile. Evolution 57, 717–745.

Blomberg, S.P., Rathnayake, S.I., Moreau, C.M., 2020. Beyond Brownian Motion and the Ornstein-Uhlenbeck Process: Stochastic Diffusion Models for the Evolution of Quantitative Characters. The American Naturalist 195, 145–165. https://doi.org/10.1086/706339

Boucher, F.C., Démery, V., 2016. Inferring Bounded Evolution in Phenotypic Characters from Phylogenetic Comparative Data. Syst Biol 65, 651–661. https://doi.org/10.1093/sysbio/syw015

Bouckaert, R., Heled, J., Kühnert, D., Vaughan, T., Wu, C.-H., Xie, D., Suchard, M.A., Rambaut, A., Drummond, A.J., 2014. BEAST 2: A Software Platform for Bayesian Evolutionary Analysis. PLoS Comput Biol 10, e1003537. https://doi.org/10.1371/journal.pcbi.1003537

Bowman, V., Ineson, J., Riding, J., Crame, J., Francis, J., Condon, D., Whittle, R., Ferraccioli, F., 2016. The Paleocene of Antarctica: Dinoflagellate cyst biostratigraphy, chronostratigraphy and implications for the palaeo-Pacific margin of Gondwana. Gondwana Research 38, 132–148. https://doi.org/10.1016/j.gr.2015.10.018

Bowman, V.C., Francis, J.E., Riding, J.B., 2013. Late Cretaceous winter sea ice in Antarctica? Geology 41, 1227–1230. https://doi.org/10.1130/G34891.1

Burls, N.J., Bradshaw, C.D., De Boer, A.M., Herold, N., Huber, M., Pound, M., Donnadieu, Y., Farnsworth, A., Frigola, A., Gasson, E., von der Heydt, A.S., Hutchinson, D.K., Knorr, G., Lawrence, K.T., Lear, C.H., Li, X., Lohmann, G., Lunt, D.J., Marzocchi, A., Prange, M., Riihimaki, C.A., Sarr, A. -C., Siler, N., Zhang, Z., 2021. Simulating Miocene Warmth: Insights From an Opportunistic Multi-Model Ensemble (MioMIP1). Paleoceanogr Paleoclimatol 36. https://doi.org/10.1029/2020PA004054

Butler, M.A., King, A.A., 2004. Phylogenetic Comparative Analysis: A Modeling Approach for Adaptive Evolution. The American Naturalist 164, 683–695.

Byrne, M., O'Hara, T. (Eds.), 2017. Australian Echinoderms : Biology, Ecology and Evolution, CSIRO Publishing. ed. Clayton.

Chapelle, G., Peck, L.S., 1999. Polar gigantism dictated by oxygen availability. Nature 399, 114–114. https://doi.org/10.1038/20097

Clavel, J., Aristide, L., Morlon, H., 2019. A Penalized Likelihood Framework For High-Dimensional Phylogenetic Comparative Methods And An Application To New-World Monkeys Brain Evolution. Systematic Biology 68, 93–116.

Clavel, J., Escarguel, G., Merceron, G., 2015. mv MORPH : an R package for fitting multivariate evolutionary models to morphometric data. Methods Ecol Evol 6, 1311–1319. https://doi.org/10.1111/2041-210X.12420

Coleman, C.O., 2007. Acanthonotozomellidae, Amathillopsidae, Dikwidae, Epimeriidae, Iphimediidae, Ochlesidae and Vicmusiidae, in: De Broyer, C. (Ed.), Synopsis of the Amphipoda of the Southern Ocean. Bruxelles, pp. 1–134.

Coleman, C.O., 2002. The transverse apodeme bridge from the cephalothorax of Amphipoda (Crustacea) and its significance for systematics. Journal of Natural History 36, 37–49. https://doi.org/10.1080/713833836

Coleman, C.O., 1991. Redescription of Anchiphimedia dorsalis (Crustacea, Amphipoda, Iphimediidae) from the Antarctic, and functional morphology of mouthparts. Zool Scripta 20, 367–374. https://doi.org/10.1111/j.1463-6409.1991.tb00301.x

Coleman, C.O., 1990. *Bathypanoploea schellenbergi* Holman & Watling, 1983, an Antarctic amphipod (Crustacea) feeding on holothuroidea. Ophelia 31, 197–205. https://doi.org/10.1080/00785326.1990.10430862

Coleman, Charles Olivier, 1989. On the nutrition of two Antarctic Acanthonotozomatidae (Crustacea: Amphipoda): Gut contents and functional morphology of mouthparts. Polar Biol 9, 287–294. https://doi.org/10.1007/BF00287425

Coleman, C. Oliver, 1989. *Gnathiphimedia mandibularis* K.H. Barnard 1930, an Antarctic amphipod (Acanthonotozomatidae, Crustacea) feeding on Bryozoa. Antartic science 1, 343–344. https://doi.org/10.1017/S0954102089000519
Coleman, C.O., Barnard, J.L., 1991. Revision of Iphimediidae and similar families (Amphipoda: Gammaridea). Proceedings of the Biological Society of Washington 104, 253–268.
Collyer, M.L., Adams, D.C., 2021. Phylogenetically aligned component analysis. Methods Ecol Evol 12, 359–372. https://doi.org/10.1111/2041-210X.13515
Colombo, M., Damerau, M., Hanel, R., Salzburger, W., Matschiner, M., 2015. Diversity and disparity through time in the adaptive radiation of Antarctic notothenioid fishes. J. Evol. Biol. 28, 376–394. https://doi.org/10.1111/jeb.12570
Crame, J.A., 2018. Key stages in the evolution of the Antarctic marine fauna. J Biogeogr 45, 986–994. https://doi.org/10.1111/jbi.13208
Crame, J.A., 2014. Evolutionary Setting, in: De Broyer, C., Koubbi, P. (Eds.), Biogeographic Atlas of the Southern Ocean. Published by The Scientific Committee on Antarctic Research, Scott Polar reseach Institute, Cambridge, pp. 32–35.
Dahl, E., 1964. The Amphipod Genus *Acidostoma*. Zoolosche Mededelingen 39, 48–58.
Dauby, Patrick, Scailteur, Y., Broyer, C.D., 2001. Trophic diversity within the eastern Weddell Sea amphipod community. Hydrobiologia 443, 69–86.
Dauby, P., Scailteur, Y., Chapelle, G., De Broyer, C., 2001. Potential impact of the main benthic amphipods on the eastern Weddell Sea shelf ecosystem (Antarctica). Polar Biology 24, 657–662. https://doi.org/10.1007/s003000100265
David, B., Saucède, T., 2015. Biodiversity of the Southern Ocean. Elsevier, Oxford.
De Broyer, C., Jazdzewska, A., 2014. Biogeographic Patterns os Southern Ocean Benthic Amphipods, in: Biogeographic Atlas of the Southern Ocean. Published by The Scientific Committee on Antarctic Research, Scott Polar reseach Institute, Cambridge, pp. 155–165.
De Broyer, C., Koubbi, P., Griffiths, H., Van de Putte, A., Raymond, B., Udekem d'Acoz, C., Danis, B., David, B., Grant, S., Gutt, J., Held, C., Hosie, G., Huettmann, F., Post, A., Ropert-Coudert, Y. (Eds.), 2014. Biogeographic Atlas of the Southern Ocean. Published by The Scientific Committee on Antarctic Research, Scott Polar reseach Institute, Cambridge.
De Broyer, C., Scailteur, Y., Chapelle, G., Rauschert, M., 2001. Diversity of epibenthic habitats of gammaridean amphipods in the eastern Weddell Sea. Polar Biology 24, 744–753. https://doi.org/10.1007/s003000100276
Dennell, R., 1933. The habits and feeding mechanism of the Amphipod Haustorius arenarius Slabber. Journal of the Linnean Society of London, Zoology 38, 363–388. https://doi.org/10.1111/j.1096-3642.1933.tb00066.x
Dolan, A.M., de Boer, B., Bernales, J., Hill, D.J., Haywood, A.M., 2018. High climate model dependency of Pliocene Antarctic ice-sheet predictions. Nat Commun 9, 2799. https://doi.org/10.1038/s41467-018-05179-4
Du Plessis, A., Broeckhoven, C., Guelpa, A., le Roux, S.G., 2017. Laboratory x-ray micro-computed tomography: a user guideline for biological samples. GigaScience 6, 1–11.
Felsenstein, J., 1985. Phylogenies and the Comparative Method. The American Naturalist 125, 1–15. https://doi.org/10.1086/284325
Frédérich, B., Sorenson, L., Santini, F., Slater, G.J., Alfaro, M.E., 2013. Iterative Ecological Radiation and Convergence during the Evolutionary History of Damselfishes (Pomacentridae). The American Naturalist 181, 94–113. https://doi.org/10.1086/668599

Fujisawa, T., Barraclough, T.G., 2013. Delimiting Species Using Single-locus Data and the Generalized Mixed Yule Coalescent (GMYC) Approach: A Revised Method and Evaluation on Simulated Datasets. Systematic Biology 62, 707–724.
Gasson, E., DeConto, R.M., Pollard, D., Levy, R.H., 2016. Dynamic Antarctic ice sheet during the early to mid-Miocene. Proc Natl Acad Sci USA 113, 3459–3464. https://doi.org/10.1073/pnas.1516130113
Gillies, C.L., Stark, J.S., Johnstone, G.J., Smith, S.D.A., 2012. Carbon flow and trophic structure of an Antarctic coastal benthic community as determined by δ13C and δ15N. Estuarine, Coastal and Shelf Science 97, 44–57. https://doi.org/10.1016/j.ecss.2011.11.003
Graeve, M., Dauby, P., Scailteur, Y., 2001. Combined lipid, fatty acid and digestive tract content analyses: a penetrating approach to estimate feeding modes of Antarctic amphipods. Polar Biology 24, 853–862. https://doi.org/10.1007/s003000100295
Harmon, L.J., Losos, J.B., Jonathan Davies, T., Gillespie, R.G., Gittleman, J.L., Bryan Jennings, W., Kozak, K.H., McPeek, M.A., Moreno-Roark, F., Near, T.J., Purvis, A., Ricklefs, R.E., Schluter, D., Schulte II, J.A., Seehausen, O., Sidlauskas, B.L., Torres-Carvajal, O., Weir, J.T., Mooers, A.Ø., 2010. Early Bursts of Body Size and Shape Evolution Are Rare in Comparative Data: Early Bursts of Evolution Are Rare. Evolution 64, 2385–2396. https://doi.org/10.1111/j.1558-5646.2010.01025.x
Harmon, L.J., Schulte II, J.A., Larson, A., Losos, J.B., 2003. Tempo and Mode of Evolutionary Radiation in Iguanian Lizards. Science 301, 961–964. https://doi.org/10.1126/science.1084786
Hayward, P.J., Ryland, J.S. (Eds.), 2017. Handbook of the marine fauna of north-west Europe, Second edition. ed. Oxford University Press, Oxford.
IAEA - International Atomic Energy Agency, n.d. IAEA-N-2 [WWW Document]. Nucleus. URL https://nucleus.iaea.org/sites/ReferenceMaterials (accessed 1.21.21a).
IAEA - International Atomic Energy Agency, n.d. IAEA-C6 [WWW Document]. Nucleus. URL https://nucleus.iaea.org/sites/ReferenceMaterials (accessed 1.21.21b).
Jerosch, K., Scharf, F.K., Deregibus, D., Campana, G.L., Zacher, K., Pehlke, H., Falk, U., Hass, H.C., Quartino, M.L., Abele, D., 2019. Ensemble Modeling of Antarctic Macroalgal Habitats Exposed to Glacial Melt in a Polar Fjord. Front. Ecol. Evol. 7, 207. https://doi.org/10.3389/fevo.2019.00207
Keklikoglou, K., Faulwetter, S., Chatzinikolaou, E., Wils, P., Brecko, J., Kvaček, J., Metscher, B., Arvanitidis, C., 2019. Micro-computed tomography for natural history specimens: a handbook of best practice protocols. EJT. https://doi.org/10.5852/ejt.2019.522
Klaus, S., Schubart, C.D., Streit, B., Pfenninger, M., 2010. When Indian crabs were not yet Asian - biogeographic evidence for Eocene proximity of India and Southeast Asia. BMC Evol Biol 10, 287. https://doi.org/10.1186/1471-2148-10-287
Konishi, S., Kitagawa, G., 1996. Generalised Information Criteria in Model Selection. Biometrika 83, 875–890.
Lagabrielle, Y., Goddéris, Y., Donnadieu, Y., Malavieille, J., Suarez, M., 2009. The tectonic history of Drake Passage and its possible impacts on global climate. Earth and Planetary Science Letters 279, 197–211. https://doi.org/10.1016/j.epsl.2008.12.037
Lawver, L., Gahagan, L., Dalziel, I., 2014. Reconstruction of the Southern Ocean and Antarctic regions, in: De Broyer, C., Koubbi, P. (Eds.), Biogeographic Atlas of the Southern Ocean. Published by The Scientific Committee on Antarctic Research, Scott Polar reseach Institute, Cambridge, pp. 36–42.
Le Bourg, B., 2020. Trophic Ecology of Southern Ocean Sea Stars. Université de Liège, Liège.

Lincoln, R.J., 1979. British Marine Amphipoda Gammaridea. British Museum Natural HistoryMineral department, London.
Linnert, C., Robinson, S.A., Lees, J.A., Bown, P.R., Pérez-Rodríguez, I., Petrizzo, M.R., Falzoni, F., Littler, K., Arz, J.A., Russell, E.E., 2014. Evidence for global cooling in the Late Cretaceous. Nat Commun 5, 4194. https://doi.org/10.1038/ncomms5194
Livermore, R., Nankivell, A., Eagles, G., Morris, P., 2005. Paleogene opening of Drake Passage. Earth and Planetary Science Letters 236, 459–470. https://doi.org/10.1016/j.epsl.2005.03.027
Lösel, P.D., van de Kamp, T., Jayme, A., Ershov, A., Faragó, T., Pichler, O., Tan Jerome, N., Aadepu, N., Bremer, S., Chilingaryan, S.A., Heethoff, M., Kopmann, A., Odar, J., Schmelzle, S., Zuber, M., Wittbrodt, J., Baumbach, T., Heuveline, V., 2020. Introducing Biomedisa as an open-source online platform for biomedical image segmentation. Nat Commun 11, 5577. https://doi.org/10.1038/s41467-020-19303-w
Lowry, J.K., Myers, A.A., 2017. A phylogeny and classification of the Amphipoda with the establishment of the new order Ingolfiellida (Crustacea: Peracarida). Zootaxa 4265, 1–89.
Lowry, J.K., Myers, A.A., 2013. A Phylogeny and Classification of the Senticaudata subord. nov. (Crustacea: Amphipoda). Zootaxa 3610, 1–80. https://doi.org/10.11646/zootaxa.3610.1.1
Lowry, J.K., Stoddart, H.E., Beesley, P.L., Houston, W.W.K., 2003. Crustacea: Malacostraca Peracarida : Amphipoda, Cumacea, Mysidacea, Zoological catalogue of Australia. CSIRO publ, Collingwood.
Mamos, T., Wattier, R., Burzyński, A., Grabowski, M., 2016. The legacy of a vanished sea: a high level of diversification within a European freshwater amphipod species complex driven by 15 My of Paratethys regression. Mol Ecol 25, 795–810. https://doi.org/10.1111/mec.13499
Mayer, G., Haug, J.T., Maas, A., Waloszek, D., 2013. Functional aspects of the gammaridean mandibles with special reference to the lacinia mobilis (Crustacea, Amphipoda). Zoologischer Anzeiger - A Journal of Comparative Zoology 252, 536–547. https://doi.org/10.1016/j.jcz.2012.11.007
Mayer, G., Maier, G., Waloszek, D., Maas, A., 2009. Mouthpart Morphology of *Gammarus roeselii* Compared to a Successful Invader, *Dikerogammarus villosus*(Amphipoda). Journal of Crustacean Biology 29, 161–174. https://doi.org/10.1651/08-3056R.1
McCutchan, J.H., Lewis, W.M., Kendall, C., McGrath, C.C., 2003. Variation in trophic shift for stable isotope ratios of carbon, nitrogen, and sulfur. Oikos 102, 378–390. https://doi.org/10.1034/j.1600-0706.2003.12098.x
McKay, R., Naish, T., Powell, R., Barrett, P., Scherer, R., Talarico, F., Kyle, P., Monien, D., Kuhn, G., Jackolski, C., Williams, T., 2012. Pleistocene variability of Antarctic Ice Sheet extent in the Ross Embayment. Quaternary Science Reviews 34, 93–112. https://doi.org/10.1016/j.quascirev.2011.12.012
Michel, L.N., Danis, B., Dubois, P., Eleaume, M., Fournier, J., Gallut, C., Jane, P., Lepoint, G., 2019. Increased sea ice cover alters food web structure in East Antarctica. Sci Rep 9, 8062. https://doi.org/10.1038/s41598-019-44605-5
Michel, L.N., D'Udekem D'Acoz, C., Frédérich, B., Léger-Bascou, L., Schön, I., Verheye, M., Lepoint, G., 2017. Effects of environmental changes on ecological niches of Iphimediidae amphipods: a stable isotope comparison of West Antarctic Peninsula and East Antarctica.
Michel, L.N., Nyssen, F.L., Dauby, P., Verheye, M., 2020. Can mandible morphology help predict feeding habits in Antarctic amphipods? Antarctic Science 32, 496–507. https://doi.org/10.1017/S0954102020000395

Miller, K.G., Wright, J.D., Katz, M.E., Browning, J.V., Cramer, B.S., Wade, B.S., Mizintseva, S.F., 2008. A View of Antarctic Ice-Sheet Evolution from Sea-Level and Deep-Sea Isotope Changes During the Late Cretaceous-Cenozoic, in: Cooper, A.K., Barrett, P.J., Stagg, H., Storey, B., Stump, E., Wise, W. (Eds.), Antaectica: A Keystone in a Changing World. Proceedings of the 10th International Symposium on Antarctic Earth Sciences, Open-File Report. The National Academies Press, Washington, D.C.

Miller, M.A., Pfeiffer, W., Schwartz, T., 2010. Creating the CIPRES Science Gateway for inference of large phylogenetic trees, in: 2010 Gateway Computing Environments Workshop (GCE). Presented at the 2010 Gateway Computing Environments Workshop (GCE), IEEE, New Orleans, LA, USA, pp. 1–8. https://doi.org/10.1109/GCE.2010.5676129

Mitteroecker, P., Gunz, P., Bernhard, M., Schaefer, K., Bookstein, F.L., 2004. Comparison of cranial ontogenetic trajectories among great apes and humans. Journal of Human Evolution 46, 679–698. https://doi.org/10.1016/j.jhevol.2004.03.006

Moore, P.G., Rainbow, P.S., 1984. Ferritin crystals in the gut caeca of *Stegocephaloides christianiensis* boeck and other stegocephalidae (amphipoda gammaridea): a functional interpretation. Phil. Trans. R. Soc. Lond. B 306, 219–245. https://doi.org/10.1098/rstb.1984.0086

Nahavandi, N., Ketmaier, V., Plath, M., Tiedemann, R., 2013. Diversification of Ponto-Caspian aquatic fauna: Morphology and molecules retrieve congruent evolutionary relationships in Pontogammarus maeoticus (Amphipoda: Pontogammaridae). Molecular Phylogenetics and Evolution 69, 1063–1076. https://doi.org/10.1016/j.ympev.2013.05.021

Naish, T., Powell, R., Levy, R., Wilson, G., Scherer, R., Talarico, F., Krissek, L., Niessen, F., Pompilio, M., Wilson, T., Carter, L., DeConto, R., Huybers, P., McKay, R., Pollard, D., Ross, J., Winter, D., Barrett, P., Browne, G., Cody, R., Cowan, E., Crampton, J., Dunbar, G., Dunbar, N., Florindo, F., Gebhardt, C., Graham, I., Hannah, M., Hansaraj, D., Harwood, D., Helling, D., Henrys, S., Hinnov, L., Kuhn, G., Kyle, P., Läufer, A., Maffioli, P., Magens, D., Mandernack, K., McIntosh, W., Millan, C., Morin, R., Ohneiser, C., Paulsen, T., Persico, D., Raine, I., Reed, J., Riesselman, C., Sagnotti, L., Schmitt, D., Sjunneskog, C., Strong, P., Taviani, M., Vogel, S., Wilch, T., Williams, T., 2009. Obliquity-paced Pliocene West Antarctic ice sheet oscillations. Nature 458, 322–328. https://doi.org/10.1038/nature07867

Near, T.J., Dornburg, A., Kuhn, K.L., Eastman, J.T., Pennington, J.N., Patarnello, T., Zane, L., Fernandez, D.A., Jones, C.D., 2012. Ancient climate change, antifreeze, and the evolutionary diversification of Antarctic fishes. Proceedings of the National Academy of Sciences 109, 3434–3439. https://doi.org/10.1073/pnas.1115169109

Nyssen, F., Brey, T., Dauby, P., Graeve, M., 2005. Trophic position of Antarctic amphipods—enhanced analysis by a 2-dimensional biomarker assay. Marine Ecology Progress Series 300, 135–145.

Nyssen, F., Brey, T., Lepoint, G., Bouquegneau, J.-M., De Broyer, C., Dauby, P., 2002. A stable isotope approach to the eastern Weddell Sea trophic web: focus on benthic amphipods. Polar Biol 25, 280–287. https://doi.org/10.1007/s00300-001-0340-0

Parnell, A.C., Phillips, D.L., Bearhop, S., Semmens, B.X., Ward, E.J., Moore, J.W., Jackson, A.L., Inger, R., 2013. Bayesian Stable Isotope Mixing Models. Environmetrics 24, 387–399.

Pasotti, F., Saravia, L.A., De Troch, M., Tarantelli, M.S., Sahade, R., Vanreusel, A., 2015. Benthic Trophic Interactions in an Antarctic Shallow Water Ecosystem Affected by

Recent Glacier Retreat. PLoS ONE 10, e0141742. https://doi.org/10.1371/journal.pone.0141742
Petersen, S.V., Dutton, A., Lohmann, K.C., 2016. End-Cretaceous extinction in Antarctica linked to both Deccan volcanism and meteorite impact via climate change. Nat Commun 7, 12079. https://doi.org/10.1038/ncomms12079
Pollard, D., DeConto, R.M., 2009. Modelling West Antarctic ice sheet growth and collapse through the past five million years. Nature 458, 329–332. https://doi.org/10.1038/nature07809
Post, A., Meijers, A., Fraser, A., Meiners, K., Ayers, J., Bindoff, N., Griffiths, H., Van de putte, A., O'Brien, P., Swadling, K., Raymond, B., 2014. Environmental Setting, in: De Broyer, C., Koubbi, P. (Eds.), Biogeographic Atlas of the Southern Ocean. Published by The Scientific Committee on Antarctic Research, Scott Polar reseach Institute, Cambridge, pp. 46–64.
Post, D.M., 2002. Using Stable Isotopes to Estimate Trophic Position: Models, Methods, and Assumptions. Ecology 83, 703–718.
Quezada-Romegialli, C., Jackson, A.L., Hayden, B., Kahilainen, K.K., Lopes, C., Harrod, C., 2018. tRophicPosition , an R package for the Bayesian estimation of trophic position from consumer stable isotope ratios. Methods Ecol Evol 9, 1592–1599. https://doi.org/10.1111/2041-210X.13009
Rabosky, D.L., Lovette, I.J., 2008. Density-dependent diversification in North American wood warblers. Proc. R. Soc. B. 275, 2363–2371. https://doi.org/10.1098/rspb.2008.0630
Register of Antarctic Marine Species (RAMS) - Iphimediidae Boeck, 1871 [WWW Document], n.d. URL https://www.marinespecies.org/rams./aphia.php?p=taxdetails&id=101387 (accessed 7.29.21).
Revell, L.J., Harmon, L.J., Collar, D.C., 2008. Phylogenetic Signal, Evolutionary Process, and Rate. Systematic Biology 57, 591–601. https://doi.org/10.1080/10635150802302427
Rutschmann, S., Matschiner, M., Damerau, M., Muschick, M., Lehmann, M.F., Hanel, R., Salzburger, W., 2011. Parallel ecological diversification in Antarctic notothenioid fishes as evidence for adaptive radiation: ECOLOGICAL DIVERSIFICATION IN NOTOTHENIOIDS. Molecular Ecology 20, 4707–4721. https://doi.org/10.1111/j.1365-294X.2011.05279.x
Sidlauskas, B., 2008. Continuous and Arrested Morphological Diversification in Sister Clades of Characiform Fishes: A Phylomorphospace Approach. Evolution 62, 3135–3156. https://doi.org/10.1111/j.1558-5646.2008.00519.x
Slater, G.J., Harmon, L.J., Alfaro, M.E., 2012. INTEGRATING FOSSILS WITH MOLECULAR PHYLOGENIES IMPROVES INFERENCE OF TRAIT EVOLUTION. Evolution 66, 3931–3944.
Søreide, J.E., Nygård, H., 2012. Challenges using stable isotopes for estimating trophic levels in marine amphipods. Polar Biol 35, 447–453. https://doi.org/10.1007/s00300-011-1073-3
Steinthorsdottir, M., Coxall, H.K., de Boer, A.M., Huber, M., Barbolini, N., Bradshaw, C.D., Burls, N.J., Feakins, S.J., Gasson, E., Henderiks, J., Holbourn, A.E., Kiel, S., Kohn, M.J., Knorr, G., Kürschner, W.M., Lear, C.H., Liebrand, D., Lunt, D.J., Mörs, T., Pearson, P.N., Pound, M.J., Stoll, H., Strömberg, C.A.E., 2021. The Miocene: The Future of the Past. Paleoceanogr Paleoclimatol 36. https://doi.org/10.1029/2020PA004037

Thatje, S., Hillenbrand, C.-D., Larter, R., 2005. On the origin of Antarctic marine benthic community structure. Trends in Ecology & Evolution 20, 534–540. https://doi.org/10.1016/j.tree.2005.07.010
Thatje, S., Hillenbrand, C.-D., Mackensen, A., Larter, R., 2008. Life Hung by a Thread: Endurance of Antarctic Fauna in Glacial Periods. Ecology 89, 682–692.
Thurber, A., 2007. Diets of Antarctic sponges: links between the pelagic microbial loop and benthic metazoan food web. Mar. Ecol. Prog. Ser. 351, 77–89. https://doi.org/10.3354/meps07122
Todini, C., Elia, A.C., Selvaggi, R., Scoparo, M., Taticchi, M.I., 2018. Food selection by *Plumatella geimermassardi* Wood and Okamura, 2004 (Phylactolaemata, Bryozoa). Knowl. Manag. Aquat. Ecosyst. 26. https://doi.org/10.1051/kmae/2018008
Uyeda, J.C., Harmon, L.J., 2014. A novel Bayesian method for inferring and interpreting the dynamics of adaptive landscapes from phylogenetic comparative data. Systematic Biology 63, 902–918.
Verheye, M., 2017. Systematics, Phylogeography and Historical Biogeography of Eusiroidea (Crustacea, Amphipoda) from the Southern Ocean, with a Special Focus on the Families Epimeriidae and Iphimediidae. Université catholique de Louvain, Louvain-la-Neuve.
Verheye, M.L., Martin, P., Backeljau, T., D'Udekem D'Acoz, C., 2016. DNA analyses reveal abundant homoplasy in taxonomically important morphological characters of Eusiroidea (Crustacea, Amphipoda). Zool Scr 45, 300–321. https://doi.org/10.1111/zsc.12153
Watling, L., 1993. Functional morphology of the amphipod mandible. Journal of Natural History 27, 837–849. https://doi.org/10.1080/00222939300770511
Watling, L., Thiel, M. (Eds.), 2013. The Natural History of the Crustacea: Functional Morphology & Diversity. Oxford University Press, Oxford ; New York.
Watling, L., Thurston, M.H., 1989. Antarctica as an evolutionary incubator: evidence from the cladistic biogeography of the amphipod Family Iphimediidae. Geological Society, London, Special Publications 47, 297–313. https://doi.org/10.1144/GSL.SP.1989.047.01.22
Wilson, D.J., Bertram, R.A., Needham, E.F., van de Flierdt, T., Welsh, K.J., McKay, R.M., Mazumder, A., Riesselman, C.R., Jimenez-Espejo, F.J., Escutia, C., 2018. Ice loss from the East Antarctic Ice Sheet during late Pleistocene interglacials. Nature 561, 383–386. https://doi.org/10.1038/s41586-018-0501-8
Wilson, G.S., Pekar, S.F., Naish, T.R., Passchier, S., DeConto, R., 2008. The Oligocene–Miocene Boundary – Antarctic Climate Response to Orbital Forcing, in: Developments in Earth and Environmental Sciences. Elsevier, pp. 369–400. https://doi.org/10.1016/S1571-9197(08)00009-8
Wilson, L.A.B., Colombo, M., Hanel, R., Salzburger, W., Sánchez-Villagra, M.R., 2013. Ecomorphological disparity in an adaptive radiation: opercular bone shape and stable isotopes in Antarctic icefishes. Ecol Evol 3, 3166–3182. https://doi.org/10.1002/ece3.708
WoRMS - World Register of Marine Species - Amphipoda [WWW Document], n.d. URL http://marinespecies.org/aphia.php?p=taxdetails&id=1135 (accessed 10.26.20).
WoRMS - World Register of Marine Species - Iphimediidae Boeck, 1871 [WWW Document], n.d. URL http://marinespecies.org/aphia.php?p=taxdetails&id=101387 (accessed 11.2.20).
Zelditch, M.L., Swiderski, D.L., Sheets, H.D., 2012. Geometric Morphometrics for Biologists: A Primer, 2nd ed. Elsevier. https://doi.org/10.1016/B978-0-12-386903-6.00001-0

Zhang, J., Liao, X.-J., Wang, K.-L., Deng, Z., Xu, S.-H., 2013. Cytotoxic cholesta-1,4-dien-3-one derivatives from soft coral Nephthea sp. Steroids 78, 396–400. https://doi.org/10.1016/j.steroids.2012.12.012

Appendix

Supplementary figure 1

Sample ID	Tree tip label	Expedition	Place	Station
ANC_DOR_03	ANC_DOR_SP1	CEAMARC	Adelie Land	8EV126
ANC_DOR_04	ANC_DOR_SP5	CEAMARC	Adelie Land	16A_EV_467_50234
ANC_DOR_N19	ANC_DOR_SP3	ANTXXIX/3	Drake Passage East	249-2
ECH_BAR_02	ECH_BAR	ANTXXIV/2	Eastern Weddell Sea	48
ECH_ECH_01	ECH_ECH_SP1	ANTXXIX/3	Bransfield Strait East	197-5
ECH_ECH_09	ECH_ECH_SP5	CEAMARC	Adelie Land	675
ECH_ECH_10	ECH_ECH_SP3	CEAMARC	Adelie Land	2519
ECH_ECH_P22	ECH_ECH_SP2	ANTXXIX/3	Bransfield Strait Joinville N	116-4
ECH_HOD_02	ECH_HOD_SP6	ANTXXIX/3	Bransfield West	224-3
ECH_HOD_03	ECH_HOD_SP1	ANTXXIX/3	Bransfield Central	199-4
ECH_HOD_08	ECH_HOD_SP2	ANTXXIX/2	Eastern Weddell Sea	48
ECH_HOD_21	ECH_HOD_SP7	REVOLTA	Adelie Land	OO2,ech17
ECH_HOD_C42	ECH_HOD_SP3	TAN0802	Western Ross Sea	100
ECH_HOD_N15	ECH_HOD_SP5	ANTXXIX/3	Weddell Erebus and Terror	162-7
ECH_IMP_P17	ECH_IMP	REVOLTA	Adelie Land	220
ECH_SCO_06	ECH_SCO	ANTXXIX/3	Weddell Volcano	185-4
ECH_WAE_06	ECH_WAE	REVOLTA	Adelie Land	07b,ech249
GNA_BAR_A8	GNA_BAR	ANTXXVII/3	Bouvet	312-3
GNA_MAN_01	GNA_MAN_SP2	CEAMARC	Adelie Land	686
GNA_SEX_01	GNA_SEX_SP1	ANTXXIX/3	Weddell Volcano	185-4
GNA_SEX_02	GNA_SEX_SP3	ANTXXIX/3	Bransfield West	227-2
GNA_SEX_20	GNA_SEX_SP2	ANTXXVII/3	Larsen B South	248-2
GNA_SEX_22	GNA_SEX_SP6	ANTXXIX/3	Bransfield Strait Joinville N	116-6
GNA_SEX_31	GNA_SEX_SP4	CEAMARC	Adelie Land	2542
GNA_SEX_C27	GNA_SEX_SP5	TAN0802	Western Ross Sea	100
GNA_SEX_O3	GNA_WAT	ANTXXIX/3	Weddell Volcano	185-4
IPH_ACU_ANT18	IPH_PAR	ANTXXIX/3	Bransfiel Strait East	197-6
IPH_BRA_N21	IPH_BRA_SP1	ANTXXI/2	Weddell Sea (Bendex)	132
IPH_BRA_P20	IPH_BRA_SP2	CEAMARC	Adelie Land	20EV490
IPH_CYC_07	IPH_CYC_SP2	ANTXXIX/3	Bransfield Strait Joinville N	116-9
IPH_CYC_20	IPH_CYC_SP1	ANTXXIV/2	Eastern Weddell Sea	48
IPH_IMP_O1	IPH_IMP	ANTXXVII/3	South of Falkland Island	208-5
IPH_MAR_07	IPH_MAR	ANTXXIII/8	Elephant Island	654-6
IPH_MIC_03	IPH_MIC	ANTXXVII/3	Weddell Sea (Bendex)	275-3
IPH_NOV_P26	IPH_NOV_1	ANTXXIV/2	Eastern Weddell Sea	48
IPH_NOV_P29	IPH_NOV_2	ANTXXIV/2	Eastern Weddell Sea	48
IPH_RIG_08	IPH_RIG_SP1	ANTXXIX/3	Bransfield Strait East	193-8
IPH_RIG_C21	IPH_RIG_SP2	TAN0802	Western Ross Sea	31
IPH_RUF_H17	IPH_RUF_SP2	CEAMARC	Adelie Land	2542
IPH_RUF_N20	IPH_RUF_SP1	ANTXXIV/2	Eastern Weddell Sea	48
LAB_PUL_C44	LAB_PUL_SP1	TAN0803	Macquarie Ridge	93
LAB_PUL_P18	LAB_PUL_SP2	CEAMARC	Adelie Land	3410
MAX_LON_03	MAX_LON_SP3	CEAMARC	Adelie Land	2200
MAX_LON_06	MAX_LON_SP1	ANTXXIX/3	Bransfield Central	204-2
MAX_LON_07	MAX_LON_SP2	ANTXXIX/3	Bransfield Strait East	197-5
PAR_INT_04	PAR_INT	CHILI	King George Island (Fildes Bay)	20110205_12
PAR_LON_O19	PAR_LON	ANTXXVII/3	Weddell Sea (Bendex)	308-1
STE_JOU_ANT22	STE_JOU_SP1	ANTXXIX/3	Weddell Volcano	185-4
STE_JOU_J18	STE_JOU_SP3	CEAMARC	Adelie Land	2519
STE_JOU_O29	STE_JOU_SP2	ANTXXIV/2	Eastern Weddell Sea	48

Date	Latitude	Longitude	Mean depth	Gear	δ13C	δ15N
27-déc-07	-66,557057	142,277252	374	NA	-18,51	14,38
14-janv-08	-66,338398	140,02921	567,9	Beam trawl	-20,32	16,84
12-mars-13	-61,93416667	-60,09266667	417	Agassiz trawl	-21,05	15,05
12-janv-08	-70,399	-8,319	598,5	Agassiz trawl	-22,03	13,95
25-févr-13	-62,7455	-57,4465	265,5	Agassiz trawl	-19,58	9,66
27-déc-07	-66,534813	141,982677	410	Beam trawl	-21,23	13,1
13-janv-08	-66,561803	141,261932	187,4	Beam trawl	-22,57	10,12
26-janv-13	-62,56316667	-56,45266667	229,9	Agassiz trawl	-21,64	11,21
04-mars-13	-63,008833	-58,5945	259	Agassiz trawl	-22,33	12,3
27-févr-13	-62,953667	-58,243333	332	Agassiz trawl	-23,04	10,66
12-janv-08	-70,399	-8,319	598,5	Agassiz trawl	-22,24	14,6
13-janv-10			30	NA	-20,14	7,91
18-févr-08	-76,202	176,248	449	Beam trawl	-23,8	15,11
10-févr-13	-63,979667	-56,770667	214,8	Agassiz trawl	-18,22	12,88
04-févr-11	-66,6333	140,0226	89	NA	-23,47	10,08
19-févr-13	-63,858833	-55,679	254	Rauschert dredge	-19,21	10,48
22-janv-10			130	NA	-22,24	12,3
09-avr-11	-54,50233333	3,225	263,5	Rauschert dredge	-23,77	11,18
26-déc-07	-66,534813	141,982677	410,3	Beam trawl	-22,7	10,98
19-févr-13	-63,858833	-55,679	254	Rauschert dredge	-19,48	8,45
05-mars-13	-62,9305	-58,684833	563	Agassiz trawl	-20,82	9,43
07-mars-11	-65,9585	-60,469167	190	Agassiz trawl	-20,73	9,65
26-janv-13			216	Rauschert dredge	-17,23	6,55
13-janv-08	-66,563722	141,255738	190,3	Beam trawl	-22,6	10,06
18-févr-08	-76,202	176,248	449	Beam trawl	-24,86	10,98
19-févr-13	-63,621333	-56,151833	254	Rauschert dredge	-20,76	6,98
25-févr-13	-62,75083	-57,44467	216	Rauschert dredge	NA	NA
12-déc-03	-70,94033333	-10,52683333	264	GSN bottom trawl	NA	NA
15-janv-08			192,5	NA	NA	NA
26-janv-13	-62,56316667	-56,4635	248,4	Agassiz trawl	-21,8	14,04
12-janv-08	-70,399	-8,319	598,5	Agassiz trawl	-23,74	9,99
11-févr-11	-54,54683333	-56,16666667	293,1	Agassiz trawl	NA	NA
29-déc-06	-61,38	-56,064	341,4	Agassiz trawl	-24,12	9,17
25-mars-11	-70,9335	-10,488	222,1	Agassiz trawl	-22,38	9,35
12-janv-08	-70,399	-8,319	598,5	Agassiz trawl	-23,9	10,61
12-janv-08	-70,399	-8,319	598,5	Rauschert dredge	NA	NA
23-févr-13	-62,728833	-57,484	429,5	Agassiz trawl	-23,5	11,22
11-févr-08	-74,5905	170,2757	283	Beam trawl	-23,61	13,52
13-janv-08	-66,563722	141,255738	190,3	Beam trawl	NA	NA
12-janv-08	-70,399	-8,319	598,5	Rauschert dredge	NA	NA
15-avr-08	-55,3533	158,4368333	605	NA	-19,74	8,15
16-janv-08			817	NA	-24,32	11,74
12-janv-08	-65,912427	143,966988	355,8	Beam trawl	-22,2	14,86
28-févr-13	-62,9345	-57,969	774	Agassiz trawl	-20,35	13,72
25-févr-13	-62,7455	-57,4465	265,5	Agassiz trawl	-20,53	15,94
05-févr-11	-62,201453	-58,960235	9	NA	-16,9	7,29
04-avr-11	-70,855	-10,58916667	237	Beam trawl	-21,59	9,75
19-févr-13	-63,85883333	-55,679	254	Rauschert dredge	-17,03	8,25
13-janv-08	-66,561803	141,261932	187,4	Beam trawl	NA	NA
12-janv-08	-70,399	-8,319	598,5	Rauschert dredge	NA	NA